Quarkonium production in high energy proton-proton and proton-nucleus collisions

Z. Conesa del Valle[a,b], G. Corcella[c], F. Fleuret[d], E.G. Ferreiro[e], V. Kartvelishvili[f], B.Z. Kopeliovich[g], J.P. Lansberg[h], C. Lourenço[b], G. Martinez[i], V. Papadimitriou[j], H. Satz[k], E. Scomparin[l], T. Ullrich[m], O. Teryaev[n], R. Vogt[o,p], J.X. Wang[q]

[a] *Institut Pluridisciplinaire Hubert Curien (IPHC), Université de Strasbourg, CNRS-IN2P3, Strasbourg, France*
[b] *European Organization for Nuclear Research (CERN), Geneva, Switzerland*
[c] *INFN, Laboratori Nazionali di Frascati, Via E.Fermi 40, I-00044, Frascati, Italy*
[d] *LLR, École polytechnique, CNRS/IN2P3, Palaiseau, France*
[e] *Departamento de Física de Partículas and IGFAE, Universidad de Santiago de Compostela, Santiago de Compostela, Spain*
[f] *Lancaster University, Lancaster LA1 4YB,United Kingdom*
[g] *Departamento de Física Universidad Técnica Federico Santa María, Instituto de Estudios Avanzados en Ciencias e Ingeniería and Centro Científico-Tecnológico de Valparaíso, Casilla 110-V, Valparaíso, Chile*
[h] *IPNO, Université Paris-Sud 11, CNRS/IN2P3, F-91406 Orsay, France*
[i] *SUBATECH, Ecole des Mines de Nantes, Université de Nantes, CNRS-IN2P3, Nantes, France*
[j] *Fermi National Accelerator Laboratory, P.O. Box 500, Batavia, Illinois, 60510, U.S.A*
[k] *Fakultät für Physik, Universität Bielefeld, Germany*
[l] *INFN Torino, Via P. Giuria 1, Torino, I-10125, Italy*
[m] *Brookhaven National Laboratory, Upton, New York 11973, USA*
[n] *Bogoliubov Laboratory of Theoretical Physics, JINR, Dubna 141980, Russia*
[o] *Physics Divsion, Lawrence Livermore National Laboratory, Livermore, CA 94551*
[p] *Physics Department, University of California at Davis, Davis, CA 95616*
[q] *Institute of High Energy Physics, Chinese Academy of Sciences, P.O. Box 918(4), Beijing, 100049, China*

Abstract

We present a brief overview of the most relevant current issues related to quarkonium production in high energy proton-proton and proton-nucleus collisions along with some perspectives. After reviewing recent experimental and theoretical results on quarkonium production in pp and pA collisions, we discuss the emerging field of polarisation studies. Thereafter, we report on issues related to heavy-quark production, both in pp and pA collisions, complemented by AA collisions. To put the work in a broader perspective, we emphasize the need for new observables to investigate quarkonium production mechanisms and reiterate the qualities that make quarkonia a unique tool for many investigations in particle and nuclear physics.

Keywords: Quarkonium, production, proton, nucleus

Contents

Operated by Fermi Research Alliance, LLC under Contract No. De-AC02-07CH11359 with the United States Department of Energy.

1. Introduction

The attention devoted to heavy quarkonium states started with the discovery of the J/ψ charmonium meson in 1974 followed by the Υ bottomonium meson in 1977. From the theoretical point of view, quarkonium bound states offer a solid ground to probe Quantum Chromodynamics (QCD), due to the high scale provided by the large mass of the heavy quarks.

The application of perturbative techniques together with the factorization principle gave birth to the Color-Singlet Model. Since then, the appearance of puzzling measurements has never stopped and has led to new challenges for theorists. These puzzles required the introduction of new ideas providing new probes for the understanding of QCD. Fifteen years ago, the observation of an excess in charmonium production reported by the CDF Collaboration, by orders of magnitude over the theoretical predictions available at that time, gave rise to the theory of Non-Relativistic QCD.

Data collected at the Tevatron, at HERA, and at low energy e^+e^- colliders has never ceased to challenge the existing theoretical models: the apparent violation of universality arising when comparing data from the hadron-hadron and the lepton-hadron colliders, the disagreement between the predictions for the polarization of the J/ψ produced in hadronic collisions and the current data, as well as the excess of double charmonium production first observed by Belle. The solution to these puzzles requires new theoretical developments on the underlying production mechanism(s), as the computation of higher-order corrections for characteristic processes and the study of new production processes, in addition to investigations of new observables not analyzed so far.

The interest in this field and its developments are not limited to the issue of the production mechanisms. The progress in lattice calculations and effective field theories have converted quarkonium physics into a powerful tool to measure the mass of the heavy quarks and the strength of the QCD coupling. The properties of production and absorption of quarkonium in a nuclear medium provide quantitative inputs for the study of QCD at high density and temperature. In fact, charmonium production off nuclei is one of the most promising probes for studying properties of matter created in ultrarelativistic heavy-ion collisions. Since quarkonium is heavy, it can be used as a probe of the properties of the medium created in these collisions, such as the intensity of interactions and possible thermalization.

Lattice QCD calculations predict that, at sufficiently large energy densities, hadronic matter undergoes a phase transition to a plasma of deconfined quarks and gluons. Since 1986, substantial efforts have been dedicated to the research of high-energy heavy-ion collisions in order to reveal the existence of this phase transition and to analyze the properties of strongly interacting matter in the new phase. The study of quarkonium production and suppression is among the most interesting investigations in this field since calculations indicate that the QCD binding potential is screened in the QGP phase. The level of screening increases with the energy density/temperature of the system. Given the existence of several quarkonium states, each of them with different binding energies, it is expected that they will sequentially melt into open charm or bottom mesons above succesive energy density thresholds. Moreover, the SPS and RHIC data on charmonium physics have brought to light further interesting results, among them puzzling features in proton-nucleus data, which highlighted new aspects of charmonium physics in nuclear reactions, namely the role of cold nuclear matter effects.

The startup of the LHC and the opening of the new energy frontier will offer new and challenging possibilities for the study of quarkonia.

All the above reasons have motivated the organization of the Quarkonium 2010 workshop held at the Ecole Polytechnique (Palaiseau, France) from July 29 to July 31, 2010. This workshop, gathering both experimentalists and theorists, was devoted to finding answers to the numerous quarkonium-hadroproduction puzzles at the dawn of the LHC era and the concurrent apogee of the Tevatron and RHIC. Introductory and review talks focusing upon recent theoretical and experimental results were presented, in addition to six topical Working Group (WG) discussion sessions, each one devoted to a specific issue:

- WG1: Quarkonium production in pp
- WG2: Quarkonium production in pA
- WG3: Polarisation and Feeddown
- WG4: Open Heavy Flavour (vs hidden)
- WG5: Quarkonium (production) as a tool
- WG6: New Observables in Quarkonium production

We present here a comprehensive review addressing all these matters. The following sections summarize the working group discussions, together with the achieved conclusions. In section 8 we prioritize directions for ongoing and future developments.

2. Quarkonium production in pp collisions

Among the wealth of quarkonium production measurements, the first CDF analyses of *direct* J/ψ and $\psi(2S)$ production[1] at $\sqrt{s} = 1.8$ TeV [1, 2] are likely the most important to date. They revealed that the measured rates were more than an order of magnitude larger than leading order (LO), color-singlet model (CSM) calculations [3], believed at that time – the mid 1990's– to be the most straightforward application of perturbative QCD to quarkonium production. Both these discrepancies motivated a number of theoretical investigations on quarkonium hadroproduction, including within the NRQCD factorization framework [4]. In the latter approach, quarkonium production can also proceed via creation of color-octet $Q\overline{Q}$ pairs, present in higher-Fock states, whose effects are believed to be suppressed by powers of the relative $Q\overline{Q}$ velocity, v.

Despite advances, there is still no clear picture of the quarkonium hadroproduction mechanisms. Such mechanisms would have to explain both the cross section and polarization measurements at the Tevatron [1, 2, 5, 6, 7, 8, 9] and at RHIC [10, 11, 12, 13, 14, 15]. Obviously, the mechanisms involved in hadroproduction should also comply with the constraints from photo/electroproduction (see [16] and references therein) and production in e^+e^- annihiliation (see [17] and references therein). Here we discuss the hadroproduction cross section only and leave the discussion of polarization to Working Group 3 (Sec. 4). We only note that the NRQCD approach, based on the dominance of the color-octet transition, so far fails to provide a consistent description of production and polarization as well as inclusive production in e^+e^- annihiliation. This failure may be because the charmonium system is too light for relativistic effects to be small and thus the velocity expansion [4] may have been truncated at too low an order. If the convergence of the velocity expansion of NRQCD is the issue, then one would expect better agreement between theory and data for the Υ. This could explain why only color-singlet contributions [18] (LO in v) appear to be in better agreement with Υ [19, 20, 21, 22] than ψ production [9].

At collider energies, quarkonium production occurs predominantly through gg channels. Higher order α_S corrections to the S states have only recently been calculated [23, 24, 25, 26, 27]. The results show that the total cross sections do not increase much when these corrections [24, 28] are included so that the perturbative series seems to converge, except perhaps at large $\sqrt{s}$ where initial-state radiation effect may need to be resummed [29]. However, the color-singlet corrections at high p_T are very large because the QCD corrections to the CSM open new production channels important at high p_T. Similar behavior has also been seen in photoproduction [30].

At LO (α_s^2), the cross section differential in p_T^2 scales as p_T^{-8} while several different diagrams which contribute at NLO decrease as p_T^{-6} or p_T^{-4}. At NLO in color-octet production, the higher-order corrections to S state production do not substantially harden the p_T distributions. The LO color octet channel, gluon fragmentation, already scales with the smallest possible power of p_T, p_T^{-4}. However, there are substantial fragmentation contributions to ${}^1S_0$ production which enhance high p_T production of these states. At NNLO (α_s^5), important new channels also appear. Color singlet gluon fragmentation is relevant in the limit $p_T \gg m$. Conversely, the exchange of two gluons in the t-channel in the high energy limit $s \gg \hat{s}$ where $s/\hat{s}$ is the square of the four-momentum of the colliding hadrons/partons has been studied in the k_T-factorization approach. In either limit, the expansion can be reorganized to simplify the evaluation of the dominant contribution. Away from this regime, corrections to each of these approaches may be important. Instead of calculating the full NNLO contributions to the CSM, NNLO* calculations consider only real gluon emission at NNLO and control the divergences using a cutoff. This method has large uncertainties arising from the sensitivity to the cutoff and the renormalization scale [18]. We briefly summarize re-

[1] "Prompt production" excludes quarkonium production from weak decays of more massive states, such as the B meson. "Direct production" further excludes quarkonium production from feeddown, via the electromagnetic and strong interactions, from more massive states, such as higher-mass quarkonium states.

cent developments here. For a more complete discussion, see Refs. [31, 32].

2.1. Current progress: Tevatron and RHIC

The contributions of the NLO color-singlet corrections reduce the discrepancy between the inclusive CSM cross sections and the CDF Υ data [9]. However, the NLO rate still falls too steeply at high p_T to describe this region successfully. The NNLO* contribution may be able to fill the gap between calculations and data at high p_T. While the large theoretical uncertainties do not place strong constraints on the color-octet contribution, the data no longer require them [32].

Higher-order color singlet contributions to J/ψ and $\psi(2S)$ production have also been calculated. The calculation is simpler for the $\psi(2S)$ because there is no feeddown from higher charmonium states. CDF extracted direct $\psi(2S)$ production [9]. The rates were compared to the CSM calculations. While the higher order CSM corrections significantly reduce the discrepancy between the calculation and the Tevatron data, they are insufficient to remove it entirely. At intermediate p_T, the upper limit of the NNLO* calculation is in agreement with the data while, for $p_T > 10$ GeV, there is a gap between the calculations and the data. The same is true for the J/ψ [32].

NLO corrections to ${}^1S_0$ and ${}^3S_1$ color octet J/ψ [27] and Υ [33] production have been calculated. In both cases, these corrections are small for $p_T < 20$ GeV. Values of the NRQCD $\langle O^{J/\psi}({}^3S_1^{[8]})\rangle$ and $\langle O^{J/\psi}({}^1S_0^{[8]})\rangle$ matrix elements were obtained by fitting the prompt production rate measured by CDF [7] and were found to be compatible with those extracted at LO [27]. Feeddown was ignored and the P state color octet contribution set to zero. Since a satisfactory fit could not be obtained for $p_T < 6$ GeV, these points were not included in the fit. Note that NRQCD factorization may break down at low p_T so that resummation effects may be necessary to describe the data in this region.

Two papers [34, 35] recently appeared with complete calculations of NLO α_s color-octet production through order v^4 for the ${}^3S_1$, ${}^1S_0$, and ${}^3P_J$ channels. Although the two calculations agree at the level of partonic cross section, the values of the NRQCD matrix elements extracted from the two different fitting procedures are inconsistent. In any case, all these computations fail to comply with the constraint obtained in [36] by assuming that the $e^+e^- \to J/\psi + X_{\text{non}-c\bar{c}}$ rate measured by Belle [37] comes *only* from the color-octet processes:

$$\langle 0|O^{J/\psi}[{}^1S_0^{(8)}]|0\rangle + 4.0\,\langle 0|O^{J/\psi}[{}^3P_0^{(8)}]|0\rangle/m_c^2 \leq (2.0 \pm 0.6) \times 10^{-2}\ \text{GeV}^3 \quad (1)$$

at NLO in α_s. If one keeps in mind that the color-singlet contribution –assumed to be zero in the equation above– saturates the experimental measurement by Belle, it is clear that this upper bound is in fact quite conservative, even though this measurement may be affected by the 4 charged track requirement. The violation of this bound by these recent NLO analyses, where color-octets dominate, should be taken rather seriously, especially because e^+e^- annihilation may be a cleaner probe of the inclusive charmonium production mechanisms.

On top of its earlier J/ψ analyses, PHENIX has shown preliminary measurements of the p_T dependence of the $\psi(2S)$ cross section at 200 GeV [14]. This is the first measurement of the p_T dependence of an excited charmonium state at RHIC. PHENIX measured the feeddown contribution of the $\psi(2S)$ to the J/ψ to be $8.6 \pm 2.3\%$, in good agreement with the world average.

STAR has recently published [13] measurements of the J/ψ cross section in 200 GeV pp collisions for $5 < p_T < 13$ GeV/c. This greatly extends the p_T range over which J/ψ data are available at RHIC. Although PHENIX can trigger at all p_T, it has so far been limited to p_T below about 9 GeV/c [14] because of its much smaller acceptance.

STAR has also recently presented a measurement of the fraction of J/ψ produced from B decays [13]. The results appear to be consistent with the CDF measurement at an order of magnitude higher energy.

Unfortunately, little is known about J/ψ feed down from higher charmonium resonances such as the χ_c at RHIC. These may significantly contribute to the yield of J/ψ mesons observed by PHENIX and STAR. For instance, it is likely that the fraction of J/ψ from χ_c should be independent of p_T, y and $\sqrt{s}$. This may be relevant for the interpretation of the high p_T STAR data [13] which favor NRQCD over CSM production in calculations with NRQCD at LO [38] and CSM contributions up to NNLO* (see [18]). Both these calculations do not include feeddown. At lower p_T, PHENIX J/ψ data [14, 15] agrees with LO NRQCD including feeddown [39]. However, in the latter case, the low p_T values may call the validity of the perturbative calculation into question, especially since the LO NRQCD spectrum diverges as $p_T \to 0$. Recently, NLO corrections to the CSM were evaluated as well and were shown to close the gap between the LO CSM and the PHENIX data at $p_T = 1 - 2$ GeV. When the NNLO* contribution is included at $p_T > 5$ GeV, the upper limit agrees with data [40]. We note here that the NLO CSM do not show any divergences at low p_T. However, resummation of initial state radiation may further improve the agreement with PHENIX data.

2.2. First LHC results

The first LHC pp run, at 7 TeV, has already produced superior quality data after a short time. The CMS [41], ATLAS [42], ALICE [43] and LHCb [44] experiments reported inclusive J/ψ p_T distributions from integrated luminosities of 100 nb^{-1}, 9.5 nb^{-1}, 11.6 nb^{-1} and 14.2 nb^{-1}, respectively. Before ALICE differential cross sections at mid-rapidity are available[2], no low p_T data will be available at mid-rapidity, see Fig. 1. ATLAS and CMS experiments are equipped with large magnetic fields, so their single muon p_T thresholds are too high for reconstruction of low p_T J/ψ's. However, the data taken at $p_T > 4$ GeV/c are consistent with each other even though the rapidity ranges differ slightly. The CMS rapidity bin, $|y| < 1.4$, overlaps the two midrapidity ranges reported by ATLAS, $|y| < 0.75$ and $0.75 < |y| < 1.5$.

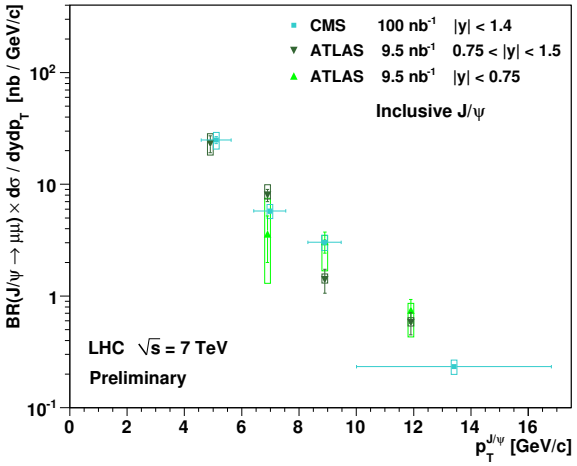

Figure 1: The preliminary mid rapidity inclusive J/ψ p_T distributions measured by CMS ($|y| < 1.4$) and ATLAS ($|y| < 0.75$ and $0.75 < |y| < 1.5$). Data compilation courtesy of H. Wöhri.

At more forward rapidities, the single muon p_T from J/ψ decay is high enough for J/ψ reconstruction at $p_T \to 0$. A compilation of the forward J/ψ data is shown in Fig. 2. The CMS and ATLAS data, taken in similar rapidity intervals of $1.4 < |y| < 2.4$ and $1.5 < |y| < 2.25$ respectively, agree rather well for $p_T > 3$ GeV/c. They seem to differ somewhat at lower p_T, but the difference is not statistically significant. The more forward LHCb and ALICE data agree quite well

[2] ALICE has released the inclusive differential p_T cross sections at large-rapidity, but only the invariant yields are available at mid-rapidity at the time of this writeup.

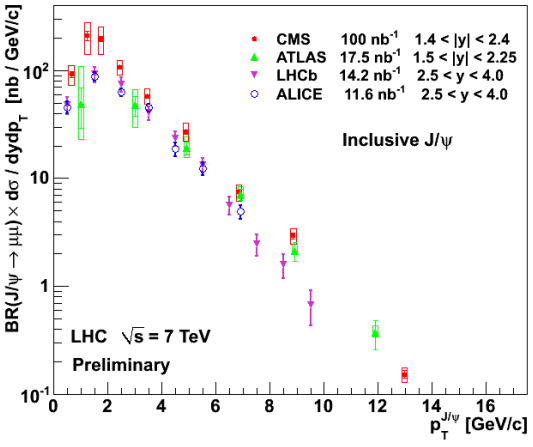

Figure 2: The preliminary forward rapidity inclusive J/ψ p_T distributions measured by CMS ($1.4 < |y| < 2.4$), ATLAS ($1.5 < |y| < 2.25$), LHCb ($2.5 < y < 4.0$) and ALICE ($2.5 < y < 4.0$). Data compilation courtesy of E. Scomparin and H. Wöhri.

with the shape of the somewhat more central rapidity CMS and ATLAS data.

The data shown in Figs. 1 and 2 are for inclusive J/ψ production which includes feeddown from the χ_c and $\psi(2S)$ states and semileptonic B meson decays. The fraction of J/ψ resulting from B meson decays,

$$B \text{ fraction} \equiv \frac{B \to J/\psi\, X}{\text{any inclusive } J/\psi} \qquad (2)$$

is compiled in Fig. 3. The preliminary LHC results at $\sqrt{s} = 7$ TeV are compared with the high statistics CDF midrapidity data [7] at $\sqrt{s} = 1.96$ TeV. The result seems to be remarkably independent of both center-of-mass energy and rapidity. The lower statistics and lower p_T STAR data also agree with the magnitude of the higher energy data shown in Fig. 3.

Although the level of the B meson contribution to J/ψ production seems to be remarkably independent of $\sqrt{s}$, the average p_T^2 of the measured inclusive J/ψ's has been seen to increase with $\sqrt{s}$. The value of both $\langle p_T \rangle$ and $\langle p_T^2 \rangle$ increases approximately linearly with ln $\sqrt{s}$ from $\sqrt{s} \sim 17$ GeV to 200 GeV. The preliminary ALICE measurement reported here [45], seems to follow this trend. The dependence of $\langle p_T^2 \rangle$ with $\sqrt{s}$ is shown in Fig. 4. Note that the fixed-target results are centered around midrapidity while two rapidity ranges, $|y| < 0.35$ and $1.2 < |y| < 2.2$, measured at RHIC, suggest that the average p_T^2 is higher at midrapidity than forward rapidity, not a surprising result. The ALICE measurement, using the muon spectrometer, is also at forward rapidity.

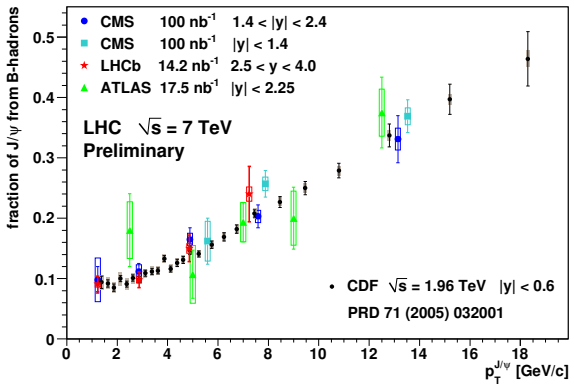

Figure 3: The preliminary fraction of non-prompt J/ψ as a function of p_T measured by CMS ($|y| < 1.4$ & $1.4 < |y| < 2.4$), ATLAS ($|y| < 2.25$) and LHCb ($2.5 < y < 4$). Data compilation courtesy of H. Wöhri.

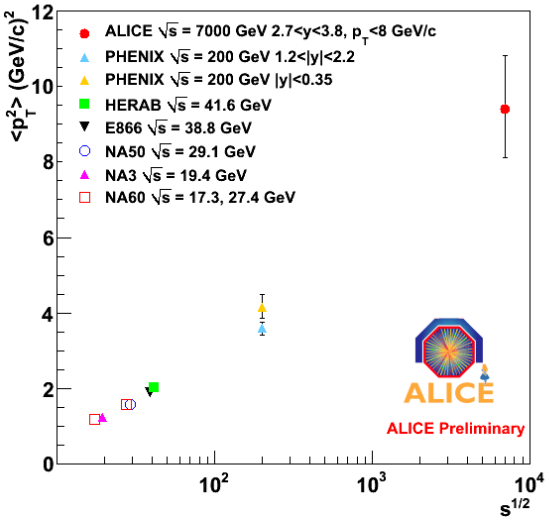

Figure 4: The preliminary measurement of $\langle p_T^2 \rangle$ from ALICE compared with lower energy data [45].

We note that comparisons of these data with model calculations using standard DGLAP evolution for the gluon distribution with perturbative QCD agree rather well (see Fig. 5 for a comparison with the CSM) suggesting that, even at rather forward rapidity, in a region of x and Q^2 where the parton densities are not well measured, no alternative factorization schemes involving *e.g.* saturation effects, are required.

Finally, CMS also reported a preliminary $\Upsilon(1S)$ measurement based on 678 ± 38 events. The $\Upsilon(1S)$, $\Upsilon(2S)$ and $\Upsilon(3S)$ peaks are clearly separated in the data.

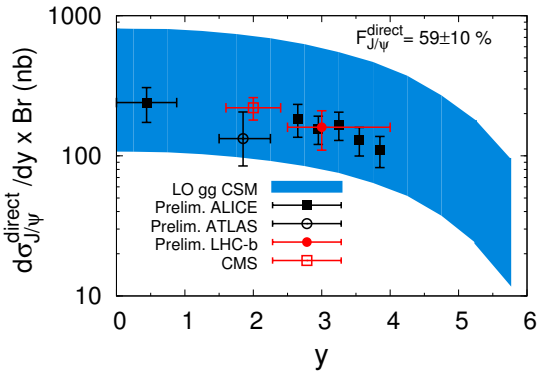

Figure 5: Comparison between the LO CSM prediction for $d\sigma^{direct}_{J/\psi}/dy \times$ Br from gg fusion LO contributions in pp collisions at $\sqrt{s}$ = 7 TeV compared to ALICE [46], ATLAS [47], CMS [48] and LHCb [49] results multiplied by the direct fraction (and correcting for the non-prompt component, assumed to be 10%, if applicable). Adapted from [29].

2.3. *What's next ?*

The LHC quarkonium data shown here is just the tip of the iceberg. More data will be forthcoming in the next runs. Presumably direct J/ψ and $\Upsilon(1S)$ production will also be measurable, *i.e.* the feeddown contributions will be distinguished and separated.

On the other hand, after September 2011, the Tevatron will unfortunately be shut down. There are 8.5 fb^{-1} of data from Run II on tape with $\sim$ 10 fb^{-1} expected by the end of the run. This should be enough data to measure the J/ψ and $\psi(2S)$ up to $p_T > 30$ GeV/c. The three Υ S states will also be measured with relatively high precision. Not only should the final Tevatron measurements include the feeddown of χ_c to J/ψ and χ_b to Υ, it is expected that the χ_c and χ_b P states with large branching ratios to the S states can be separated from each other using photon conversions. Even though Run II will come to an end, the data will continue to be analyzed for some time with more exciting results forthcoming.

HERA has already ended its physics run. However, analyses are still in progress. The H1 and ZEUS data have been combined in these final analyses, increasing the available statistics. These fits will better improve our understanding of quarkonium photoproduction.

Indeed, utilizing the entire Tevatron and HERA data sets to study the balance between production of color

singlet and color octet states in hadro- and photoproduction will provide more insight into the production mechanisms than fitting to either data set alone. Last but not least, the B-factory analyses on charmonium production, not only from B decays, are detailed enough nowadays to separate out the different inclusive contributions, imposing constraints on the production mechanisms at B factories, ep colliders and pp colliders. For instance, it starts to be rather clear that $C = +1$ color-octet transitions are much less probable than initially thought, which suppresses the leading color-octet yield at $p_T < 5$ GeV in hadroproduction.

In 200 GeV pp collisions, PHENIX has measured cross sections for production of the (unresolved) Υ states and the $\psi(2S)$. A χ_c measurement will be published soon. All of these measurements involve low yields and will benefit greatly from improved luminosity in the next few years. PHENIX has also measured the polarization of the J/ψ in 200 GeV pp collisions and will also do so with existing 500 GeV data. PHENIX and STAR will also produce unpolarized J/ψ and Υ results at 500 GeV, a new energy midway between the 200 GeV data and the Tevatron energy.

RHIC is vigorously pursing a long term plan of detector and machine upgrades. The ongoing RHIC luminosity upgrades will be completed by the 2013 run. The introduction in 2011 and 2012 of silicon vertex detectors into PHENIX at mid and forward rapidity and of the STAR Heavy Flavor Tracker in 2014, will enable open charm and open bottom to be measured independently with greatly improved precision. The detector upgrades will also allow improved measurements of quarkonium states due to improved mass resolution and background rejection.

The RHIC run plan for the next 5 years or so will be centered on exploiting the capabilities of the new silicon vertex detectors and other upgrades, combined with the increased RHIC luminosity. There will likely be long pp runs at 200 GeV, plus shorter runs at 62 GeV to explore the energy dependence of open and hidden heavy flavor production. The luminosity increase and the PHENIX detector upgrades will enhance the PHENIX heavy quarkonium program with increased p_T reach for the J/ψ and low statistics measurements of the combined Υ states. The increased luminosity will enable the large acceptance STAR detector to extend its p_T reach to considerably higher values for Υ and J/ψ measurements than previously possible.

The RHIC program for the period beyond about 5 years is still under development. The RHIC experiments are presently engaged in preparing a decadal plan that will lay out their proposed science goals and detector upgrades for 2011 to 2020.

3. Quarkonium production in pA collisions

The study of charmonium production is an interesting test of our understanding of strong interaction physics. For pp collisions, various theoretical approaches have been proposed, but a satisfactory description of J/ψ hadroproduction is still missing [31]. In spite of this situation, the study of quarkonium production in the apparently more difficult proton-nucleus environment has also attracted considerable interest. In fact, in pA, the heavy-quark pair is created in the nuclear medium, and the study of its evolution towards a bound state can add significant constraints to the models. For example, the strength of the interaction of the evolving $c\bar{c}$ pair with the target nucleons, that can lead to a break-up of the pair and consequently to a suppression of the J/ψ yield, may depend on its quantum states at the production level (color-octet or color-singlet), and on the kinematic variables of the pair [50, 51]. In addition to final-state effects, also initial-state effects may influence the observed J/ψ yield in pA. In particular, parton shadowing in the target nucleus [52, 53, 54, 55, 56] may suppress (or enhance, in case of antishadowing) the probability of producing a J/ψ, and its effect depends on the kinematics of the $c\bar{c}$ pair production [57]. Moreover, the energy loss in the nuclear medium of the incident parton [58], prior to $c\bar{c}$ production, may significantly alter the J/ψ cross section and its kinematic distribution. Finally, a suppression of the J/ψ has been proposed a long time ago as a signature of the formation, in ultrarelativistic nucleus-nucleus collisions, of a state where quarks and gluons are deconfined (Quark-Gluon Plasma) [59]. Results from pA collisions, taken in the same kinematical conditions of AA, and properly extrapolated to nucleus-nucleus collisions, can be helpful to calibrate the contribution of the various cold nuclear matter effects to the overall observed suppression [60, 61].

3.1. Basic phenomena and observables

3.1.1. Hierarchy of time scales

Nuclear effects are controlled by the characteristic time scales of charmonium production. A colorless $\bar{c}c$ pair created in a hard reaction is not yet a physical charmonium state since it does not have a fixed mass. According to the uncertainty relation it takes time to disentangle the ground state charmonium from its excitations,

$$t_f = \frac{2E_{\bar{c}c}}{m^2_{\psi'} - m^2_{J/\psi}}. \quad (3)$$

This time scale can be also interpreted as formation time of the charmonium wave function. At charmonium energies $E_{\bar{c}c} < 25$ GeV in the nuclear rest frame this time is shorter than the mean nucleon spacing in a nucleus, $t_f < 2$fm, so one can treat the formation process as instantaneous, and the attenuation in nuclear matter is controlled by the inelastic charmonium-nucleon cross section,

$$S(L) = \exp\left[-\sigma_{in}^{J/\psi N} L \rho_A\right], \tag{4}$$

where L is the path length in the medium of density ρ_A.

At much higher energies, $E_{\bar{c}c} \gg 100$ GeV, the formation time is long, $l_f \gg R_A$, even for heavy nuclei, the initial size of the $\bar{c}c$ dipole is "frozen" by Lorentz time dilation during propagation through the nucleus, so the attenuation factor gets the simple form,

$$S(L) = \langle \exp\left[-\sigma(r_T) L \rho_A\right] \rangle_{r_T}, \tag{5}$$

where the exponential is averaged over transverse separation r_T of the dipole weighted with the initial and final distribution amplitudes [50]. This regime is relevant for J/ψ production at RHIC at the mid rapidity, where $E_{\bar{c}c} = 300$ GeV. The J/ψ energy rises with y as e^y relative to the target nucleus, but decreases as e^{-y} relative to the beam nucleus. Therefore, the asymptotic regime is relevant to any positive rapidity in dA collisions, but in AA collisions at forward rapidities nuclear effects turn out to be in different regimes for the two colliding nuclei.

Another important time scale characterizes the hard process of $\bar{c}c$ pair creation. Although the proper time is short, $t^* \sim 1/m_c$, it is subject to Lorentz time dilation in a frame, where the charm quarks have high energy.

$$t_c = \frac{2E_{\bar{c}c}}{M^2_{\bar{c}c}} \tag{6}$$

If this time is short, $t_c < 2$ fm, one can consider production as instantaneous. This regime corresponds to charmonium energy $E_{\bar{c}c} < 50$ GeV. This estimate is relevant for production of χ, but the characteristic energy may be about twice higher for J/ψ, because in the color singlet model the invariant mass of $\bar{c}c$ is $\langle M^2_{\bar{c}c} \rangle = 2m^2_{J/\psi}$. This time scale is usually short for J/ψ produced at mid rapidity in fixed-target experiments. For instance at $\sqrt{s} = 40$ GeV $t_c = 1.2$ fm if $x_F = 0$.

The most difficult for calculations is the intermediate energy regime, where either t_c or/and t_f are of the order of the nuclear size. Theoretical tools for this case, the path-integral technique, was developed in [50, 62]. The $\bar{c}c$ dipole is produced with a separation $\sim 1/m_c$ and ends up with the large size of J/ψ. The time scale for such an expansion, t_f, rises with energy, therefore the effective absorption, or break-up, cross section is expected to drop with energy [50]. Indeed, this effect was observed in fixed target experiments, as is plotted in Fig. 6. Data are well explained by color transparency for expanding $\bar{c}c$ dipoles.

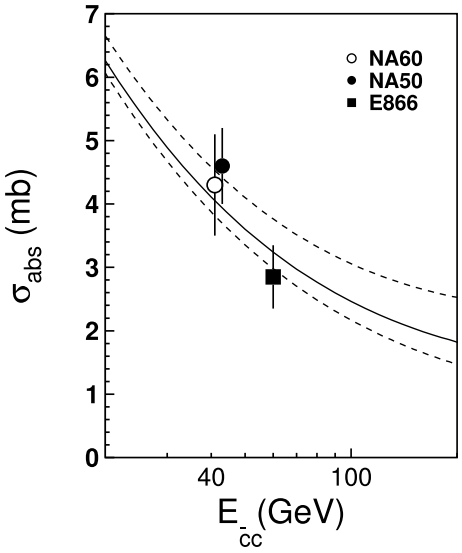

Figure 6: The effective break-up cross section as function of J/ψ energy. The solid curve shows theoretical expectation [62]. The dashed curves show the estimated theoretical uncertainty.

3.1.2. Higher twist charm quark shadowing

In the regime of long time scale for $\bar{c}c$ production, of $t_c \gg R_A$, the process, $g \to \bar{c}c$, is subject to shadowing. This is apparently higher twist, since the mean $\bar{c}c$ transverse separation is $\langle r_T \rangle \sim 1/m_c$. Same is true for the break-up cross section of the produced colorless $\bar{c}c$ propagating through the nucleus.

The amplitude of $\bar{c}c$ production at a point with impact parameter b and longitudinal coordinate z, averaged over the dipole size, reads [63, 64],

$$S_{pA}(b,z) = \int d^2 r_T \, W_{\bar{c}c}(r_T) \times \exp\left[-\frac{1}{2}\sigma_{\bar{c}cg}(r_T) T_-(b,z) - \frac{1}{2}\sigma_{\bar{c}c}(r_T) T_+(b,z)\right]. \tag{7}$$

Here $T_-(b,z) = \int_{-\infty}^{z} dz' \rho_A(b,z')$; $T_+(b,z) = T_A(b) - T_-(b,z)$, and $T_A(b) = T_-(b,\infty)$. Shadowing for $\bar{c}c$ production over the nuclear thickness $T_-(b,z)$ occurs with the shadowing cross section corresponding to a 3-body dipole, gluon and $\bar{c}c$, which for equal momenta of c and $\bar{c}$ equals to $\sigma_{\bar{c}cg}(r_T) = \frac{9}{4}\sigma_{\bar{c}c}(r_T/2) - \frac{1}{8}\sigma_{\bar{c}c}(r_T)$.

For $t_c \gg R_A$ the weight factor in (7) has the form [63], $W_{\bar{c}c}(r_T) \propto K_0(m_c r_T)\, r_T^2\, \psi_{J/\psi}(r_T)$, where one factor r_T comes from the amplitude of $\bar{c}c$ production, and another one either from the amplitude of gluon radiation in the case J/ψ production, or from the radial wave function of χ_2.

With the survival probability amplitude Eq. (7) the nuclear ratio reads,

$$R_{pA} = \frac{1}{A} \int d^2b \int_{-\infty}^{\infty} dz \left| S_{pA}(b,z) \right|^2 . \qquad (8)$$

The results at $\sqrt{s} = 200$ GeV are plotted by dashed curve in Fig. 7 as function of y. [64].

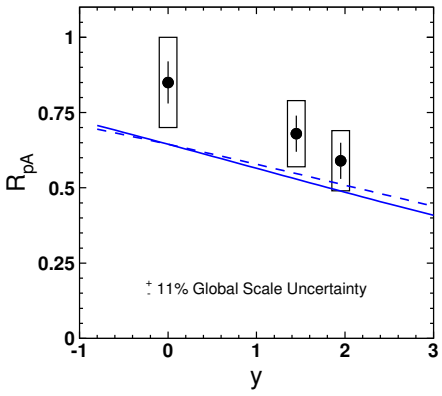

Figure 7: Dashed curve presents nuclear suppression of J/ψ as function of rapidity in pA collisions. Solid curve is corrected for gluon shadowing. Data are for dAu collisions at $\sqrt{s} = 200$ GeV [65].

3.1.3. *Leading twist gluon shadowing*

In terms of the Fock state decomposition gluon shadowing corresponds to higher Fock components in the projectile hadron, containing at least one gluon. Multiple interactions of this gluon in the nuclear target are the source of shadowing.

Theoretical expectations for gluon shadowing are quite diverse. A weak shadowing was predicted within the dipole approach [66] and in an analysis [52] of DIS data developed at leading and next-to-leading order – nDS LO and NLO parameterizations[3] –. However, a rather strong shadowing and correspondingly antishadowing for gluons was evaluated in [67] based on the hadronic representation [68, 69] and in the global analyses EKS98 [53, 54], EPS08 [55] and EPS09 [56]. We emphasize that the two last analyses included data on proton-nucleus collisions, which makes them model dependent. We finally note that nDSg and EKS98 parameterizations are compatible for $x < 10^{-3}$.

Also, the choice of the adequate partonic production mechanism – either via a $2 \to 1$ or a $2 \to 2$ process – may affect both the way to compute the nuclear shadowing and its expected impact on the production [57].

This controversy should be settled after nuclear effects for charmonium production at LHC will be studied experimentally.

3.1.4. *Non trivial transition from pA to AA*

The usual strategy in search for a signal of final state attenuation of charmonia in the created dense medium, is extrapolation to AA collisions of the cold nuclear matter effects observed in pA. This is how the "anomalous" suppression of J/ψ was observed in the NA50/60 data [70, 71, 72, 73, 74]: one fits the effective absorption cross section σ_{abs} to describe the nuclear suppression observed in pA collisions. Some results of such a procedure are shown in Fig. 6. Then with this cross section one predicts the normal cold nuclear matter effects in nuclear collisions, and whatever deviates from such an expectation is called anomalous and is related to the final state suppression.

However, recent data [75] from the NA60 experiment for p_T broadening of J/ψ depicted in Fig. 8 demonstrate that such an extrapolation may not be straightforward, since the "cold" nuclear matter in AA collisions turns out not to be cold at all.

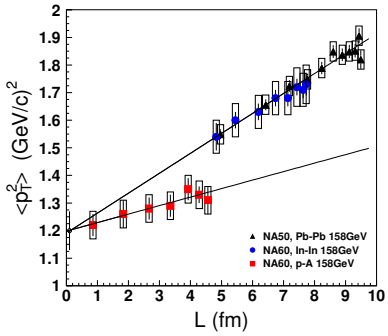

Figure 8: J/ψ p_T broadening measured at SPS as a function of the path length L in nuclear matter.

Indeed, broadening, Δp_T^2, is known to be proportional to the path length in the medium and its density. The data show that broadening observed in nucleus-nucleus

[3] We note that the same DIS analysis provided a constrained NLO fit with a stronger gluon shadowing – nDSg –. The χ^2 of this fit is however not as good as that of the unconstrained fit –nDS.

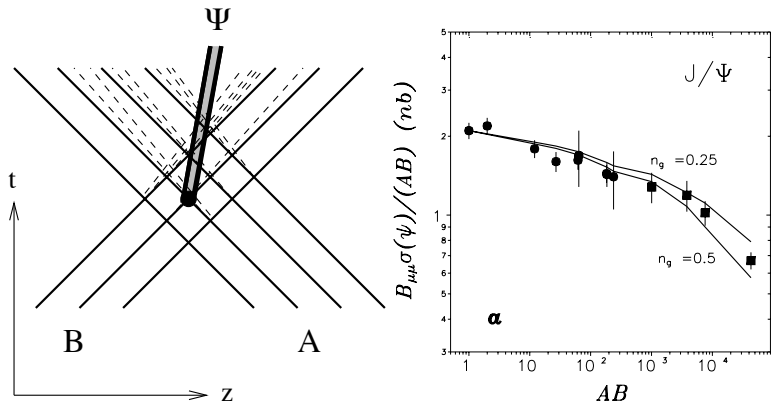

Figure 9: *Left:* A two-dimensional (time - longitudinal coordinate) plot for charmonium production in a collision of nuclei A and B in the c.m. of the colliding nucleons. The solid and dashed lines show the nucleon and gluon trajectories, respectively. *Right:* Nuclear suppression of J/ψ production in pA and AB collisions as function of the product $A \times B$. The two curves demonstrate theoretical uncertainty of calculations [76]. The circles and squares correspond to pA and AB data, respectively. The data points are from [70, 71, 72].

collisions is twice as large as in pA for the same total path length. This means that the cold nuclear matter is twice as dense in AA compared to pA collisions. Correspondingly, the effective absorption cross section σ_{abs} should be taken twice bigger when one makes predictions for AA collisions. Such a significant enhancement of absorption effects may explain the observed anomalous suppression.

This effect was successfully predicted in [76] as a result of multiple NN collisions and gluon radiation preceding their interaction with the J/ψ (or $\bar{c}c$ dipole), as is illustrated in the left panel of Fig. 9.

It was also shown that quantitatively this effect is able to explain the observed anomalous J/ψ suppression, as is depicted in the right panel of Fig. 9. Simultaneously, the same effect of increased medium density leads to a significant increase of broadening in AA compared to pA collisions.

Suppression of J/ψ caused by gluon radiation decreases as $1/\sqrt{s}$ and vanishes at high energies of RHIC and LHC. However, at the energies of LHC broadening of J/ψ is expected to be highly enhanced in AA compared to pA collisions for another reason.

Notice that observation of an anomalously large broadening has an important advantage compared to anomalous suppression. While the latter may originate from either initial, or final state interactions, which can be easily mixed up, the former comes entirely from initial state multiple interactions. Indeed, a colorless $\bar{c}c$ dipole attenuates in a medium, but does not have any energy loss and does not change its momentum. Note that the partonic process may affect this result [77].

3.1.5. Transverse momentum broadening

The mean transverse momentum squared of heavy quarkonia increases in pA collisions compared to pp. The magnitude of the effect, $\Delta p_T^2 = \langle p_T^2 \rangle_A - \langle p_T^2 \rangle_p$ is usually called broadening. Broadening of a parton propagating through a nuclear medium can be calculated within the dipole approach as [78, 79],

$$\Delta p_T^2 = 2\, C(E) \int_0^L dz\, \rho_A(z), \tag{9}$$

where the factor $C(E)$ is related to the dipole-proton cross section $\sigma_{\bar{q}q}(r_T)$ known from phenomenology. For broadening of gluons

$$C_g = \frac{9}{8}\, \vec{\nabla}^2_{r_T}\, \sigma_{\bar{q}q}(r_T)\Big|_{r_T=0}. \tag{10}$$

Using the dipole cross section in the saturated form fitted to DIS data [80, 66] one can predict the factor $C_g(E)$ and broadening Eq. (9). The results depicted in Fig. 10 by dashed curves well agree with data for J/ψ and Υ. Inclusion of gluon shadowing corrections reduces the amount of shadowing, but within the error bars.

One should also understand the p_T dependence of the cross section and the energy dependence of the mean value $\langle p_T^2 \rangle$, depicted in Fig. 11.

Remarkably, data on pp, pA and even AA collisions, at the energies of fixed target experiments and at RHIC [65], are described well by the simple parametrization,

$$\frac{d\sigma}{dp_T^2} \propto \left(1 + \frac{p_T^2}{6\langle p_T^2 \rangle}\right)^{-6}. \tag{11}$$

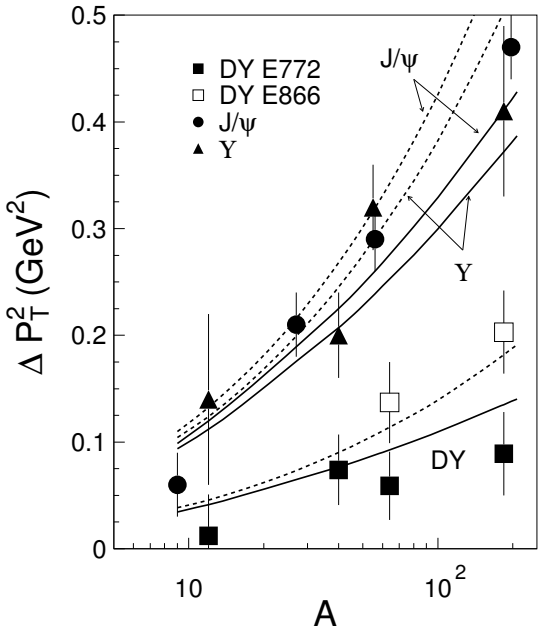

Figure 10: Broadening for J/ψ and Υ [81] is shown by circles and triangles respectively. The dashed and solid curves correspond to the predictions based on Eq. (9) without and with the corrections for gluon shadowing respectively.

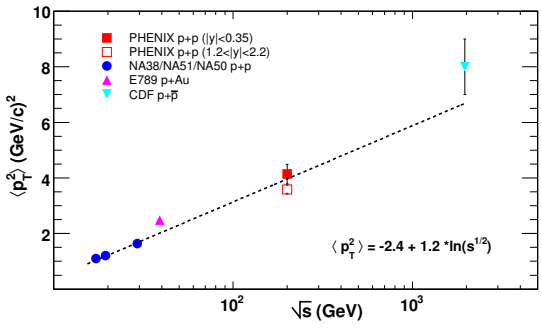

Figure 11: The J/ψ $\langle p_T^2 \rangle$ in pp collisions as function of energy. Data are from [10].

If one considers that broadening does not alter the shape of the p_T-distribution of produced J/ψ, the simplest way to calculate the p_T-dependence of the pA cross section is just making a shift Δp_T^2 in the mean value $\langle p_T^2 \rangle$ for pA compared to pp. The resulting A-dependence of the pA over pp ratio, R_{pA}, is presented in Fig. 12 as function of p_T in comparison with data [82] at $\sqrt{s} = 39$ GeV. The A-dependence is parametrized as $R_{pA} = A^{\alpha-1}$, and $\alpha(p_T)$ is plotted in Fig. 12.

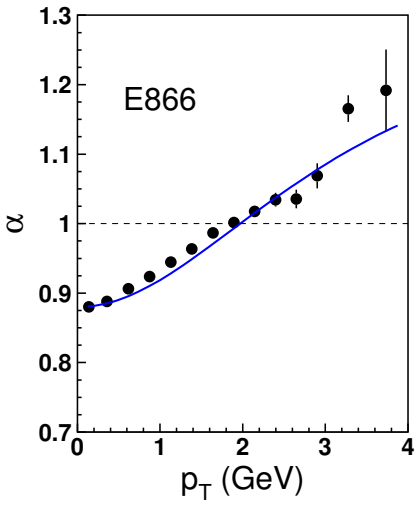

Figure 12: The exponent $\alpha = 1 + \ln(R_{pA})/\ln(A)$ as function of p_T calculated with Eq. (11) in comparison with data from [82].

3.1.6. *Feynman x_F dependence of nuclear effects*

Available data on x_F-dependence of nuclear effects in charmonium production demonstrate increasing nuclear suppression towards large x_F, as is shown in Fig. 13, for the exponent $\alpha(x_F)$ characterizing the A-dependence, $\sigma_{pA}^{J/\psi} \propto A^{\alpha}$.

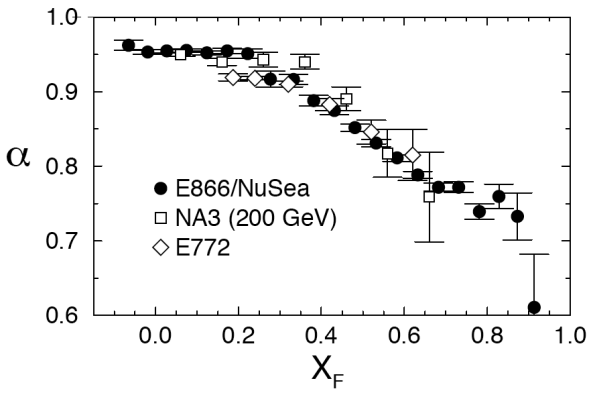

Figure 13: The exponent $\alpha(x_F)$ characterizing the A-dependence, $\sigma_{pA}^{J/\psi} \propto A^{\alpha}$ at $\sqrt{s} = 39$ GeV [82] an $\sqrt{s} = 20$ GeV [83].

Although several mechanisms contributing to the J/ψ suppression have been proposed, there is still no comprehensive description so far of the observed x_F-dependence of the nuclear effects. The first mechanism proposed in [84] explored initial state energy loss independent off the collision energy, according to pQCD calculations, or string model. However, a finite energy loss becomes insignificant at high energies, while data

in Fig. 13 demonstrate an approximate x_F scaling. Apparently, the energy loss must be proportional to the initial energy, in order to provide an x_F-scaling. Such an energy loss was ad hoc introduced in [58], and was criticized later in [85], as contradicting perturbative QCD calculations.

The observed x_F-dependence of nuclear suppression was interpreted in [86] in terms of the Fock state decomposition as the energy sharing problem enhanced by the nucleus towards the kinematic limit. This mechanism also explains a similar suppression observed at large x_F in many other reactions, Drell-Yan process, high and low p_T production of different species of hadrons, etc.

Attempts to explain the observed suppression to gluons shadowing, as a dominant mechanism, was not successful. That would lead to x_2 scaling, which is severely broken in data [81].

3.2. Existing measurements and future perspectives

3.2.1. Fixed-target experiments

Since in charmonium production in pA a rather complicated interplay of various physical processes occurs, the availability of accurate sets of data, spanning large intervals in the incident proton energy, and covering large x_F and p_T regions, is essential for a thorough understanding of the involved mechanisms. At fixed target energies, high-statistics J/ψ samples have been collected in recent years by the DESY experiment HERA-B [87], at 920 GeV incident energy, by E866 [88] at FNAL at 800 GeV, by the CERN-SPS experiment NA50 at 400 and 450 GeV [89] and by the NA60 experiment at 158 and 400 GeV [90]. Usually, nuclear effects have been parametrized by fitting the A-dependence of the production cross section with the simple power law $\sigma^{pA}_{J/\psi} = \sigma^{pp}_{J/\psi} \cdot A^{\alpha}$, and then studying the evolution of α with x_F and p_T. Alternatively, nuclear effects have been expressed by fitting the data in the framework of the Glauber model [91], having as input parameters the inelastic nucleon-nucleon cross section and the density distributions for the various nuclei [92]. The model gives as an output the so-called J/ψ absorption cross section $\sigma^{abs}_{J/\psi}$. Clearly, both α and $\sigma^{abs}_{J/\psi}$ represent effective quantities, including the contribution of the various sources of nuclear effects sketched in the previous section.

The results for α as a function of x_F are summarized in Fig. 14, and show various remarkable features. First of all one can note a steady increase in the strength of nuclear effects (α decreases) when increasing x_F. More in detail, the decrease of α at large x_F has usually been attributed to energy loss of the projectile partons and indeed various models have tried to explain, at least qualitatively, such an effect (see e.g. [93] and more recently [77]). On the other hand an important constraint on the size of parton energy loss comes from experiments studying nuclear effects on Drell-Yan production. At this workshop [94], it has been shown that the initial-state parton energy loss needed to describe the NA3 data on Drell-Yan production [95] is too small (by a factor 5 to 10) to explain at the same time the observed high-x_F suppression for J/ψ. Therefore, a quantitative assessment of this effect is still lacking. At the other extreme of the explored x_F region (negative values), one observes a slight tendency towards enhancement of the J/ψ production ($\alpha > 1$). In this region a model [96] formulated in the framework of reggeon phenomenology, indeed predicts an anti-screening effect, which cannot be reproduced by more conventional approaches based on the commonly used shadowing parameterizations.

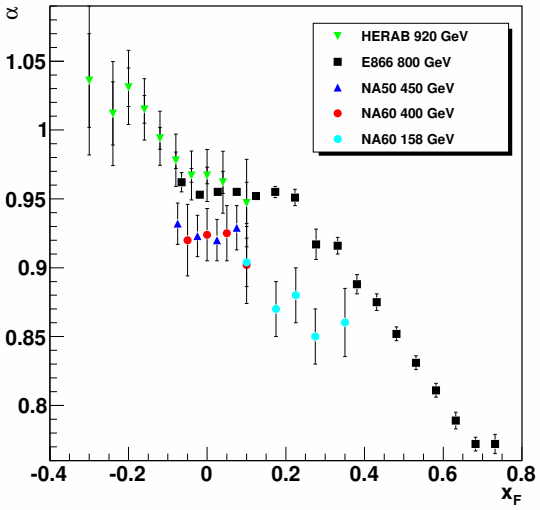

Figure 14: Compilation of experimental results on α vs x_F.

At midrapidity, several experiments have studied J/ψ production. The most remarkable feature is a tendency towards stronger nuclear effects when $\sqrt{s}$ of the pA interaction decreases. In this region, the relevant processes affecting the production should be the final-state breakup of the $c\bar{c}$ pair and the parton shadowing in the nuclear target. Both processes should approximately scale with x_2, i.e. one would expect nuclear effects to be the same at a certain x_2 independently of the initial proton energy. However, recent results by NA60 [97], comparing α as a function of x_2 for J/ψ production at

158 and 400 GeV, show that such a scaling does not hold, and that therefore other mechanisms should be invoked to explain the $\sqrt{s}$-dependence of nuclear effects at midrapidity.

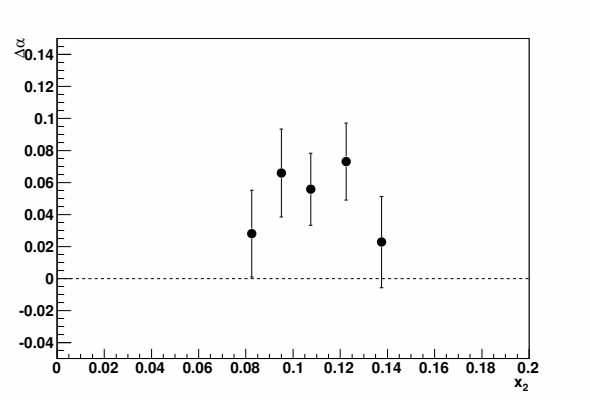

Figure 15: $\Delta\alpha$=$\alpha_{400\mathrm{GeV}} - \alpha_{158\mathrm{GeV}}$ vs x_2, as measured by NA60 in pA collisions at 158 and 400 GeV.

To summarize, in spite of the rather extended set of measurements, which clearly define a trend for nuclear effects on J/ψ production, the interpretation of fixed-target observations still remains unsatisfactory. For the future, further results obtained at lower energies, at the SPS or at the future FAIR facility, may help produce a better characterization of the evolution of nuclear effects vs $\sqrt{s}$. First ideas for fixed-target measurements at *higher* $\sqrt{s}$ [98], using proton beams extracted from the LHC, are also under consideration.

3.2.2. Collider experiments

The study of J/ψ production and propagation in cold nuclear matter has also been carried out at RHIC energies, through dAu collisions. The conclusions from the first round of measurements from the PHENIX experiment were not so sharp [65], because of the limited available statistics, but this problem has been recently overcome, with the availability of a first set of results corresponding to a much larger data sample (Run-6). One of the key features of the PHENIX results is the large rapidity coverage, including positive and negative rapidities, corresponding to a large range of relative momenta between the $c\bar{c}$ pair and the medium.

More in detail, PHENIX has recently released dAu R_{CP} data for J/ψ production [14] in nine rapidity bins over $|y| < 2.4$. Systematic uncertainties associated with the beam luminosity, detector acceptance, trigger efficiency, and tracking efficiency cancel when R_{CP}, the ratio of central to peripheral events, normalized to the number of NN collisions, is formed. There is a remaining systematic uncertainty due to the centrality dependence of the tracking and particle identification efficiencies.

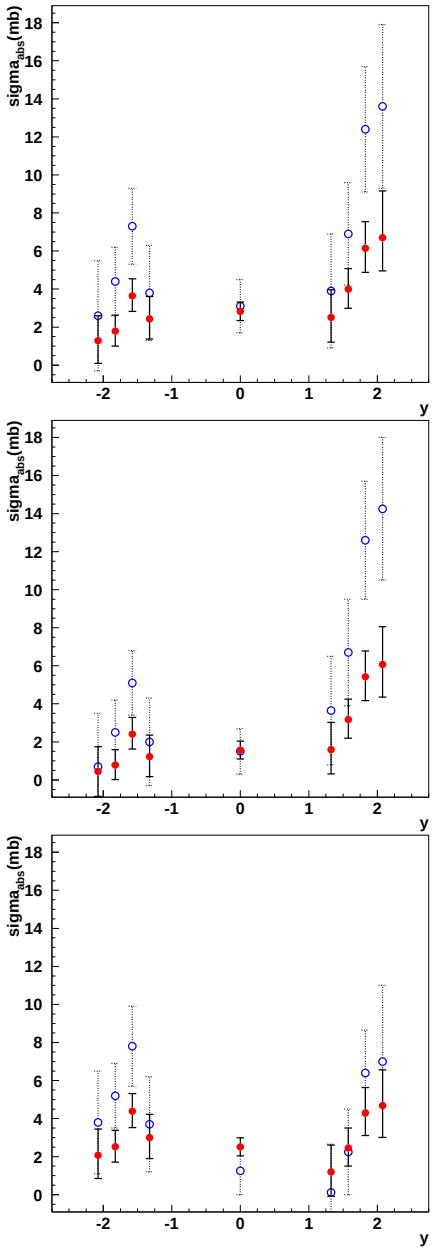

Figure 16: The effective absorption cross section as a function of rapidity extracted from PHENIX dAu R_{CP} data in the extrinsic $2 \rightarrow 2$ scheme [102] (in red closed circle) compared to the $2 \rightarrow 1$ scheme [99] (in blue open circle) using a) EKS98, b) EPS08 and c) nDSg. From [102].

More importantly, there are significant systematic uncertainties in the centrality dependence of R_{CP} due to the

use of a Glauber model to calculate the average number of nucleon-nucleon collisions as a means of estimating the relative normalization between different centrality bins. The systematic uncertainty due to the Glauber calculation is independent of rapidity.

The PHENIX dAu R_{CP} data have been independently fitted at each of the nine rapidities [99] employing a model including shadowing and J/ψ absorption. The model calculations [100] use the EKS98 and nDSg shadowing parameterizations with $0 \leq \sigma^{abs}_{J/\psi} \leq 15$ mb. The best fit absorption cross section was determined at each rapidity, along with the $\pm 1\sigma$ uncertainties associated with a) rapidity-dependent systematic uncertainties and b) rapidity-independent systematic uncertainties. The most notable feature is the stronger effective absorption cross section at forward rapidity, similar to the behavior observed at lower energies [88]. In fact, it is striking that the extracted cross sections at forward rapidity are very similar for PHENIX ($\sqrt{s_{NN}} = 200$ GeV) and for the E866 collaboration ($\sqrt{s_{NN}} = 38.8$ GeV) [101], despite the large difference in center-of-mass energy. One should note the large global systematic uncertainty in $\sigma_{\rm abs}$ extracted from the PHENIX R_{CP} data, dominated by the uncertainty in the Glauber estimate of the average number of collisions at each centrality. Although it does not affect the shape of the rapidity dependence of $\sigma^{\rm abs}_{J/\psi}$, it results in considerable uncertainty in the magnitude of the effective absorption cross section.

It was recently suggested [57, 102] that the large increase in effective absorption cross section at forward rapidity obtained from a LO CEM calculation [99], may be significantly moderated if a more accurate $2 \rightarrow 2$ kinematics is used. Figure 16 shows the results from the $2 \rightarrow 1$ kinematics [99], compared to the ones from a $2 \rightarrow 2$ kinematics [102] using the s-channel cut [103] as partonic model. The difference emphasizes the importance of understanding the underlying production mechanisms.

PHENIX has very recently released [104] final $R_{d\rm Au}$ and R_{CP} data from the 2008 dAu RHIC run (where $R_{d\rm Au}$ is the J/ψ yield in dAu collisions normalized to the pp yield times the number of NN collisions). The final R_{CP} data are in very good agreement with the preliminary results described above. A comparison of the $R_{d\rm Au}$ data with the R_{CP} data shows that a simultaneous description of the two observables will require a stronger than linear dependence of the J/ψ suppression on the nuclear thickness function at forward rapidity. The dependence of the suppression on nuclear thickness is at least quadratic, and is likely higher. This result may have important implications for the understanding of forward-rapidity dAu physics, as well as for the estimate of cold nuclear matter effects in AuAu collisions.

3.2.3. Cold nuclear matter effects at LHC energy

The new energy regime recently opened up by the advent of the LHC offers new possibilities for the study of quarkonium in cold nuclear matter. However, although the study of pA collisions is foreseen in the LHC physics program, the details of the acceleration scheme and the choice of the nuclear beam still have to be finalized. Consequently, the study of the physics observables accessible to the experiments is still at a rather preliminary level. Clearly, pA data at the LHC are essential to investigate various physics effects, and "in primis" nuclear shadowing in a still unexplored x-range. The final-state interaction of charmonia with cold nuclear matter is another attractive topic. Due to the expected very short overlap time of the heavy-quark pair with nuclear matter, one could expect its influence on the still almost point-like $c\bar{c}$ to be very small. However, these considerations are very qualitative and deeper theoretical studies are clearly necessary.

At this workshop, preliminary studies carried out in the frame of the ALICE experiment have been discussed [105]. In particular, the availability of a forward muon spectrometer (rapidity coverage $2.5 < y < 4$) gives the opportunity for studying effects connected with gluon saturation via the measurement of $R_{p\rm Pb}$ for the J/ψ. A model for heavy-quark production in a Color-Glass Condensate environment [106] has been used to make predictions for $R_{p\rm Pb}$ as a function of y and p_T in the acceptance of the ALICE muon spectrometer. Such predictions quantitatively differ from the expectations related to a pure shadowing scenario, making such a measurement an interesting tool to investigate saturation-related effects.

4. Polarisation and feed-down in quarkonium production

Until recently, the numerous puzzles in the prediction of quarkonium-production rates at hadron colliders were attributed to non-perturbative effects associated with channels in which the heavy quark and antiquark are produced in a colour-octet (CO) state [107, 108, 109, 110]. It is now widely accepted that α_s^4 and α_s^5 corrections to the CSM [3] are fundamental for understanding the p_T spectrum of J/ψ and Υ produced in high-energy hadron collisions [24, 23, 25, 26, 18, 32]. The effect of QCD corrections is also manifest in the polarisation predictions. While the J/ψ and Υ produced

inclusively or in association with a photon are predicted to be transversally polarised at LO via a color singlet (CS), it has been recently emphasised that their polarisation at NLO is increasingly longitudinal when p_T gets larger [25, 18, 127, 128].

On the other hand, the LO NRQCD calculation (for which CO transitions dominante) predicts a sizable transverse polarisation rate for large p_T J/ψ [111, 112, 113, 114, 115] whereas the Tevatron CDF measurement at Fermilab [8] displays a slight longitudinal polarisation at large p_T for J/ψ and Υ and a stronger one for $\psi(2S)$.

To clarify the situation, more efforts on both experimental and theoretical aspects are expected from the forthcoming LHC. In the following, we review important aspects of quarkonium polarisation both from a theoretical and experimental perspective with particular emphasis on the $J = 1$ states such as the J/ψ, $\psi(2S)$ and $\Upsilon(nS)$.

4.1. Frames and polarizations

The polarisation of the $J = 1$ quarkonia is defined from their dilepton decay. In general, the angular distribution of the dilepton is

$$W(\vartheta,\varphi) \propto \frac{1}{(3+\lambda_\vartheta)}(1+\lambda_\vartheta\cos^2\vartheta+\lambda_\varphi\sin^2\vartheta\cos 2\varphi + \lambda_{\vartheta\varphi}\sin 2\vartheta\cos\varphi), \tag{12}$$

where ϑ and φ are the (polar and azimuthal) angles of the positive lepton with, respectively, the polarisation axis z and the production plane xz (containing the colliding particles and the decaying meson). Several polarisation frames have been used in the past. In the helicity frame the polar axis coincides with the flight direction of the meson in the centre-of-mass frame of the colliding hadrons. In the Collins-Soper frame, the polar axis reflects, on average, the direction of the relative velocity of the colliding partons.

To clarify this puzzling situation, improved measurements are needed. So far, most experiments have presented results based on a fraction of the physical information derivable from the data: only one polarisation frame is used and only the polar projection of the decay angular distribution is studied. These incomplete results prevent model-independent physical conclusions. Moreover, such partial descriptions of the observed physical processes reduce the chances of detecting possible biases induced by insufficiently controlled systematic effects. In the forthcoming LHC measurements, it is important to approach the polarisation measurement as a multidimensional problem, determining the full angular distribution in more than one frame.

In a series of recent works [116, 117, 118, 119], a frame-invariant formalism was proposed to minimize the dependence of the measured result on the experimental acceptance. It provides a much better control of the systematic effects due to detector limitations and analysis biases. The overall idea is to study both experimentally and theoretically the quantity

$$\tilde{\lambda} = \frac{\lambda_\vartheta + 3\lambda_\varphi}{1-\lambda_\varphi}, \tag{13}$$

instead of λ_ϑ and λ_φ.

4.2. Charmonium polarization

The NLO QCD corrections to J/ψ polarisation in the CSM at Tevatron and LHC have been calculated for the first time in [25]. At order α_S^4, one should also take into account the contribution for $gg \to J/\psi + c\bar{c}$ [23]. These are dominant at large p_T. The results showed that the J/ψ polarisation changes drastically from strongly transverse at LO into strongly longitudinal at NLO. While, this does not completely agree with the CDF data, the trend is rather encouraging especially since feed-down from P-waves can alter the prompt yield polarisation. The same trend is observed for the $\psi(2S)$ [32], for which polarization measurements are not affected by the P-waves. This is illustrated by Fig. 17.

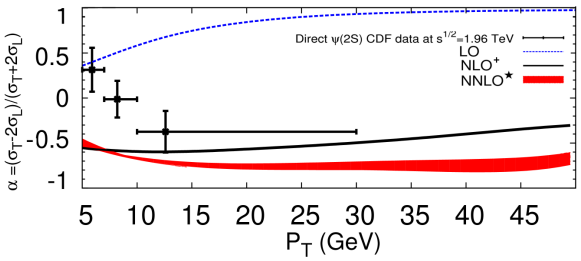

Figure 17: Polarisation of $\psi(2S)$ directly produced as function of its transverse momentum p_T at the Tevatron as predicted by the CSM at LO, NLO$^+$ (including $gg \to J/\psi c\bar{c}$) and at NNLO* compared to the CDF measurement at $\sqrt{s} = 1.96$ TeV.

The first NLO QCD corrections of the J/ψ production via CO states $[^1S_0^{(8)}, {}^3S_1^{(8)}]$ at the Tevatron and LHC were studied in [27]. Contrary to the CS case, these corrections only slightly change the J/ψ p_T distributions and the polarisation compared to the LO NRQCD calculations. This result implies that the perturbative QCD expansion quickly converges for J/ψ production via the S-wave CO state, in contrast to the CSM, where

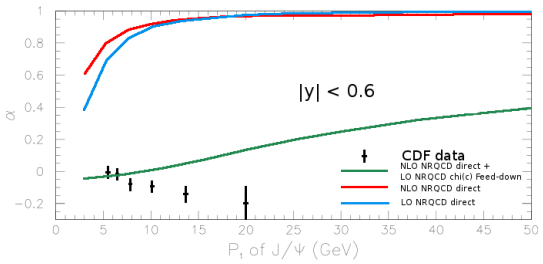

Figure 18: Direct-J/ψ yield polarisation α based on the work [27] and the NRQCD matrix elements are from the recent work [34]. The experimental data is from the CDF measurement at the Tevatron [8] for the prompt J/ψ.

the NLO contributions open new channel which show a leading p_T behaviour with a different J/ψ polarisation.

As shown in Fig. 4.2, an obvious gap between the theoretical results for J/ψ polarisation calculated up to NLO including CO transition [27] and the experimental measurements at Tevatron is observed for increasing p_T. There still remains only a narrow window which might fill the gap if one follows the *a priori* rigourous theoretical framework of NRQCD, namely the NLO corrections to J/ψ production via P-wave CO states and J/ψ production by feed down from χ_{cJ}. It is worth noting however that the latter possible solution does not apply for $\psi(2S)$ where a similar gap is observed –with a large magnitude even–, while the former one would be at odds with the suppression of $C = +1$ CO transition expected from e^+e^- studies.

The results given by two recent works [34, 35, 120] show that the p_T distribution of the P-wave CO contribution at QCD NLO can be decomposed into the linear combination of the two S-wave COs. In Ref. [34], the χ_c feed down to prompt J/ψ hadroproduction is taken into account, contributing at the level of $20-40\%$. In this case, the NRQCD matrix elements $\langle O_n^H \rangle$ are determined to be $\langle O_8^\psi(^3S_1)\rangle = 0.0005$ GeV^3 and $\langle O_8^\psi(^1S_0)\rangle = 0.076$ GeV^3. It should be noted that some experimental data have been omitted since the fit of the p_T distribution starts at 7 GeV. The theoretical prediction for the polarisation of the direct J/ψ hadroproduction is plotted in Fig. 18, based on the calculation of Ref. [27]. We also note that such a value for $\langle O_8^\psi(^1S_0)\rangle$ does comply with the constraint of Eq. (1). This either hints at an overestimation of this transition in these studies or at a breaking of NRQCD matrix-element universality for charmonia. In such a case, NRQCD would become nearly unpredictive as far as charmonium production is concerned.

Two aspects should be emphasized when comparing the theoretical prediction and the existing experimental measurements. It is impossible to give the polarisation of the prompt J/ψ hadroproduction without a calculation of the polarisation for the χ_c feed-down contribution if it really contributes $20-40\%$ to the p_T distribution. In addition, the polarisation prediction in Fig. 18 for direct J/ψ production assumes that the CO $^3P_J^{[8]}(J/\psi)$ NRQCD matrix element can be neglected. If not, its contribution to J/ψ polarisation must calculated at NLO accuracy. At LO, the χ_c and the P-wave CO contributions were both taken into account in the first NRQCD-based predictions [113].

4.3. Bottomonium polarization

As regards the polarisation of Υ produced in pp collisions, the NLO CSM correction was first presented in [26], and followed by an analysis including the real-emissions at NNLO [18] which we discuss later on. The polarization is quite similar to that of J/ψ, *i.e.* the polarisation changes drastically from strongly transverse at LO into strongly longitudinal at NLO. The NLO results are also rather similar to those obtained in the k_T factorisation approach at LO [121, 122].

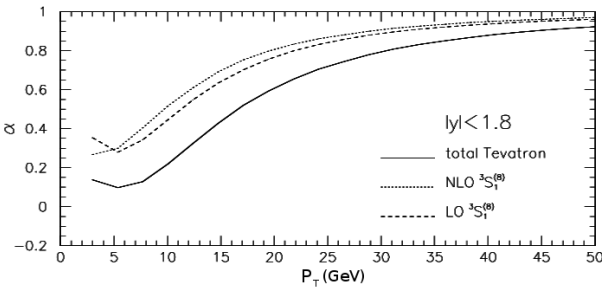

Figure 19: Transverse momentum distribution of polarization parameter α for direct Υ production at the Tevatron.

The NLO QCD corrections of the Υ production via CO $[^1S_0^{(8)}, ^3S_1^{(8)}]$ at the Tevatron and the LHC were studied for the first time in [33]. The Υ polarization parameter, α, from CO $[^3S_1^{(8)}]$ as function of p_T is shown in Fig. 19. Slight changes can be observed when the NLO corrections are taken into account. For any p_T, the direct Υ yield from CO is transversally polarized, with $\alpha > 0.5$ as soon as $p_T > 10$ GeV. The predictions for the polarization of Υ production when the CSM NLO yield is added are also presented in the figure as a "total" result.

In Fig. 20, the polarization of inclusive (*i.e.* prompt) Υ production at the Tevatron is shown. As the polarization of Υ from the feed-down of $\chi_b(nP)$ is not available yet, a huge band is obtained only by imposing that the polarization of this part is between -1 to 1. The experimental data from D0 and CDF is also shown in the same

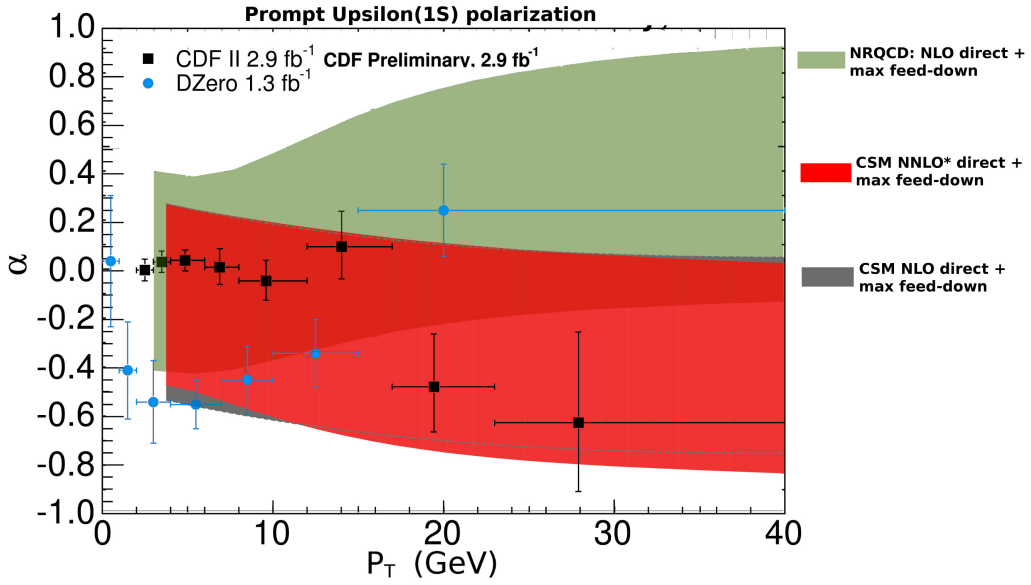

Figure 20: Extrapolated prompt $\Upsilon(1S)$ polarization as a function of its transverse momentum at the Tevatron as predicted by NRQCD (including CO transitions) [33], CSM at NLO [18] and CSM at NNLO* [18], compared to the D0 [22] and CDF [123] data.

figure. Since both data sets clearly disagree, it is difficult to draw any strong conclusion from such a comparison. Yet, if one follows the CDF analysis based on a higher integrated luminosity and where the 3 Υ states are clearly separated out, one observes the same gap opening with p_T as for the ψ's, even with such a large theoretical uncertainty. For the sake of completeness, one should underline that the direct yield from CO transitions is always predicted to be transverse. The CO yield can only become slightly longitudinal thanks to the (unknown) feed-down. This is a clear motivation for the CDF and D0 to measure the polarisation of direct $\Upsilon(1S)$ or that of $\Upsilon(3S)$, the latter being *de facto* direct.

In addition to the evaluation of the NLO CSM contributions to Υ production, a subset of the NNLO contributions were evaluated in [18], these are the real-emission contribution at order α_S^5 believed to provide the leading contribution at large p_T. It was indeed found that these contributions, included in the NNLO* yield, could be large and bring an agreement between a CSM-based evaluation and the CDF data. It also occured that the NNLO* yield showed the same polarisation than the NLO yield, excepted for the –important– fact that the yield was correctly described. The polarization of directly-produced Υ predicted likewise does not agree with the experimental data since it is strongly longitudinally polarized. Nevertheless, as we have discussed above, the experimental data includes contributions from P-wave decays, up to roughly 40 %, and these can decay into transversally polarised $\Upsilon(1S)$. Even if the feed-down yield is unpolarized, the prompt polarization would only be 0.6 times the direct polarization. Clearly when this is taken into account, the CSM NNLO* and the NLO agree with the CDF data, as depicted by the gray (labeled NLO) and red (labeled NNLO*) band of Fig. 20.

In this partial QCD NNLO calculation, some infrared divergences are not automatically regulated since the loop corrections at α_s^5 are missing. This imposed the introduction of an infrared cut-off, whose effect is believed to decrease as p_T increases, provided that the real-emissions dominates at large p_T. This may not be exactly realised if double t-channel gluon exchanges have an important impact. In this case, the result could be overestimated. However, the agreement with the k_T factorisation results gives us the hope that the infrared divergences are for a large part under control.

This partial QCD NNLO calculation was also applied to the J/ψ and the $\psi(2S)$ case [32] and the contribution was also found to be important. Yet, contrary to the Υ case, there is still a small gap opening at large p_T. At the leading order in v, the prediction for the J/ψ and the $\psi(2S)$ are identical. The $\psi(2S)$ polarisation as function of p_T is depicted by the red band (labeled NNLO*) band of Fig. 17. It is similar to that of NLO.

4.4. Polarization in photoproduction and at RHIC

The J/ψ polarization in photoproduction at HERA was also studied up to NLO in [124, 125]. The results showed that the transverse momentum, p_T, and energy fraction, z, distributions of J/ψ production do not agree well with the observations. The theoretical uncertainties on the z distributions of the J/ψ polarization parameters in the target frame for various choices of the renormalization and factorization scales are too large to provide a definite prediction relative to the experimental data [126]. It is quite easy to understand that the uncertainty in the QCD effects could be rather large since the p_T of the J/ψ is quite small at HERA, $1 < p_T < 5$ GeV. Thus the theoretical prediction is not expected to agree well with the measurements.

The NLO CSM polarisation of the J/ψ produced in proton-proton collisions at RHIC at $\sqrt{s} = 200$ GeV has been studied [40]. The results show that the polarisation pattern at NLO in the helicity frame is in good agreement with the PHENIX data both in the central [15] and the forward [12] regions when extra contribution from cg fusion and a data-driven range for the χ_c contribution to the J/ψ polarisation are considered. For the time being, nothing is known about P-wave feed downs at RHIC especially at large p_T where x_T starts to be large. This prevents any strong conclusion based on the comparison with the data regarding the status of the CO contributions and a possible overestimation by the partial NNLO contribution.

4.5. Perspectives on polarization studies

To clarify the J/ψ polarisation puzzle, other observables such as the measurements of J/ψ (Υ) hadroproduction in association with a photon at the LHC can be considered. The NLO CS contribution was studied [127] and the results show that the J/ψ polarization changes from transverse at leading-order to longitudinal at NLO. It is known that the CO contribution to the inclusive J/ψ hadroproduction may be one order of magnitude larger than the CS contribution, and the polarization distribution may be dominated by the CO at NLO. In contrast, the CS contribution for $J/\psi + \gamma$ production is at least of the same order as the CO contribution. The polarization should then arise from both the CS and CO. Therefore, measurements of J/ψ production associated with a direct photon at hadron colliders could be an important test of the theoretical treatment of heavy-quarkonium production. The partial NNLO result [128], NNLO*, is about one order of magnitude larger than the NLO J/ψ p_T distribution. The predicted polarization are almost the same. Therefore, it will be reality check on the partial NNLO treatment.

Moreover, to compare the polarisation measurements in different frames, we need theoretical predictions based on different polarisation frames such as the helicity frame (HX) and Collins-Soper frame. Along these lines, we would like to mention a recent pioner work on the polarization studies of $\Upsilon + \gamma$ in the k_T factorization approach using different polarization frames [129].

Theoretical predictions of the new, proposed, frame-independent polarisation parameter $\tilde{\lambda}$ are needed. Of course, all the prediction should at NLO accuracy. Furthermore, the comparison between experimental data and theory must consider the experimental acceptance and efficiency. Experiments measure the net polarisation of the specific cocktail of quarkonium events accepted by the detector, trigger and analysis cuts. It will be very useful to have an event generator where the quarkonium decay into lepton pairs for inclusive production at NLO which could be embedded into Monte Carlo simulations.

5. Open heavy-flavor production in *pp* and *pA* collisions

Open heavy-flavor production in pp and pA collisions is tightly connected to the process of quarkonium (hidden flavor) production. Nevertheless, it is in itself one of the most interesting processes to study from theoretical and experimental points of view (see, e.g., Refs. [130, 131] for a review on recent results). In fact, the production of heavy quarks allows us to test fundamental concepts, such as perturbative QCD, factorization and non perturbative power corrections. It also represents a mandatory benchmark for quarkonium production and parameters derived in open heavy-flavor production serve as the basis for calculations of quarkonium production.

Thanks to the massiveness of heavy quarks, the production cross section can be calculated analytically in perturbative QCD down to $p_T = 0$ at the partonic level [132]. However, differential distributions and event shapes exhibit large logarithmic contributions, typically corresponding to soft or collinear parton radiation, which need to be resummed to all orders [133, 134, 135]. Furthermore, dead-cone effects suppress gluon radiation around the heavy-quark direction, which has relevant phenomenological implications on both parton- and hadron-level spectra. As far as heavy-hadron production is concerned, one can model non perturbative effects by means of a fragmentation function, depending on a few tunable parameters, or by including power corrections in a 'frozen' or 'effective' strong coupling constant [136, 137, 138]. Reliable

hadronization models should also be capable of distinguishing the spin of the produced hadrons, e.g. separating the D^* from the D, and describing both baryons and mesons and the multiplicity ratios Λ_c/D or Λ_b/B. Typically, hadronization models, such as the cluster [139] or string [140] models, are implemented within the framework of Monte Carlo generators, such as HERWIG [141], PYTHIA [142] or MC@NLO [143] and are tuned to heavy-hadron data from e^+e^- experiments, e.g. LEP and SLD data (see, for example, [144] for a tuning to b-quark fragmentation). Multi-purpose generators have been available for several years for lepton/hadron collisions in the vacuum and have been lately modified to include the effects of dense matter [145, 146] (see also [147, 148, 149, 150, 151] for generators specific for heavy-ion collisions).

A profound knowledge of open heavy-quark production is crucial for the understanding of quarkonium phenomenology. The production, e.g., of the J/ψ in Non relativistic QCD (NRQCD) is described as the convolution of the perturbative $c\bar{c}$ cross section and a non perturbative operator, possibly depending on the color of the $c\bar{c}$ state, according to the color-singlet and color-octet mechanisms (see e.g. [152]).

In order to promote the formalism used to describe open heavy flavors to pA and ultimately AA collisions, one has to introduce medium-modification effects, taking into account the existing differences between light and heavy quarks (hadrons) [153]. In particular, one of the most striking observations of heavy-ion collisions is the jet-quenching phenomenon, namely the suppression of hadron multiplicity at large transverse momentum (p_T) with respect to pp processes [154, 155, 156, 157].

In the case of heavy hadrons, the measured suppression is expected to be lower than that of light-flavor mesons, due to the dead-cone effect discussed above. This effect becomes less important in the high-p_T limit where $p_T \gg m_Q$. So far, suppression of heavy-flavored mesons in pA or AA collisions has only been measured through leptons, i.e., the non-photonic electrons and muons from semi leptonic decays of heavy-flavored mesons [158, 159, 160]. Despite being a rather complex study, non-photonic electrons and muons have various experimental advantages, the most important one being the possibility to deploy the fast triggers, in such a way to allow the experiments to collect large data samples. On the other hand, they originate from both charm and bottom mesons with only few indirect experimental handles available to disentangle the two contributions.

Suprisingly, the energy loss observed through non-photonic electrons is substantial already at moderate p_T of ~3 GeV/c. Figure 21 shows this suppression via the nuclear modification factor R_{AA} defined as the ratio of invariant yields in AuAu over that in pp collisions times the number of binary nucleon collisions in the AuAu system at a given centrality. In the absence of any nuclear or dense matter effects R_{AA} is unity. Several mechanisms to describe heavy-flavor energy loss in the dense medium have been so far proposed. Most prominent are collisional and radiative energy loss, typically calculated in the weak-coupling regime. However, the magnitude of the observed suppression at RHIC is hard to accommodate in these models. Recent attempts, assuming strong coupling between the heavy-flavor mesons and the dense medium, and based on the AdS/CFT correspondence, lead to higher suppression factors, but further studies and experimental data are needed before any conclusions can be drawn.

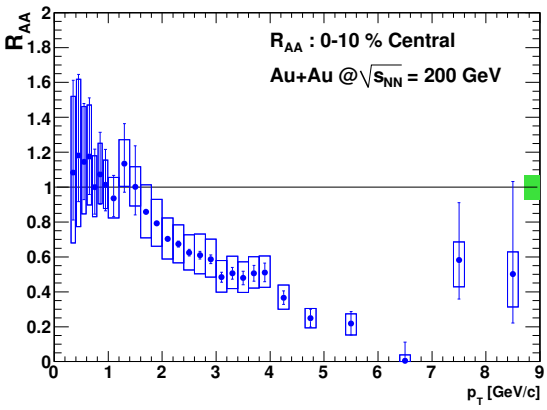

Figure 21: Nuclear modification factor (R_{AA}) for non-photonic electrons originating from semileptonic decays of heavy-flavored mesons in the 0-10% most central AuAu collisions at RHIC measured by PHENIX [158]. This corresponds to the ratio of the invariant yields in AuAu and pp collisions normalized by the number of binary nucleon collisions. This measurement indicates a strong suppression of heavy-flavored mesons in central heavy-ion collisions.

It is still an open question to what extent the energy-loss mechanisms, observed in open heavy-flavor production, affect the quarkonium yields in AA collisions. After including quark-antiquark recombination effects, the quenching of open heavy-flavored hadrons will also serve as a benchmark for quarkonia in heavy-ion collisions.

Another crucial issue in heavy-flavor phenomenology concerns heavy-quark parton distributions in protons and nuclei. In fact, processes with the production of heavy quarks are fundamental to constrain the PDFs. Higher-order corrections to the production of heavy quarks, with the implementation of soft/collinear resummation to improve the differential distributions,

will also be helpful to acquire information on heavy quark densities. The possible inclusion of medium effects in the hard-scattering cross section, along with nuclear parton distribution functions, will eventually lead to a prediction taking fully into account the modifications induced by the dense matter. However, unlike collisions in the vacuum, there is no guarantee that factorization should also work in a medium.

In the following, we shall review the main results discussed within the Open Heavy-Flavor Working Group in the Quarkonium 2010 workshop. We shall discuss higher-order calculations of heavy-flavor production spectra at RHIC, taking particular care about the role played by the resummation on transverse-momentum distributions. We shall then present a few selected topics on specific features of heavy quarks and dead-cone effects, as well as novel developments on the modelling of energy loss from heavy quarks in dense matter and its possible relation with the jet-quenching observation. Later on, recent results on the production of photon plus heavy quarks, along with its relevance to constrain charm/bottom PDFs in proton and heavy ions, will be investigated.

5.1. *Open heavy-flavor production at RHIC and FONLL calculations*

As our understanding of heavy-ion collisions becomes more mature, it becomes increasingly clear that heavy-flavor studies are a mandatory tool to further our understanding of the quark-gluon-plasma formed in high energy nuclear collisions at RHIC and now at LHC. Having reliable measurements of all aspects of heavy-flavor production is compelling.

Experimentally, the total charm cross section is not well constrained. Measurements of charm meson production at the Tevatron could be conducted only at large transverse momenta ($p_T > 5$ GeV/c) while measurements at lower energies exhibit rather large uncertainties. At RHIC, measurements of D mesons in conjunction with low-p_T non-photonic electrons and muons in dAu collisions [161] (STAR) indicate a rather large total charm cross section of ~1.3 mb. On the other hand, the non-photonic lepton measurements in pp collisions [158] (PHENIX) suggest a considerably smaller cross section of ~ 0.6 mb. In all cases assumptions about rapidity distributions and contributions from unmeasured charm mesons and baryons (e.g. Λ_c) have to be made, adding further contributions to the already large statistical and systematic uncertainties. Upgrades to the existing RHIC detectors (for an overview see [162]) will help to overcome these shortcomings. A summary of current total charm cross sections ($\sigma_{c\bar{c}}$) is presented in Fig. 22.

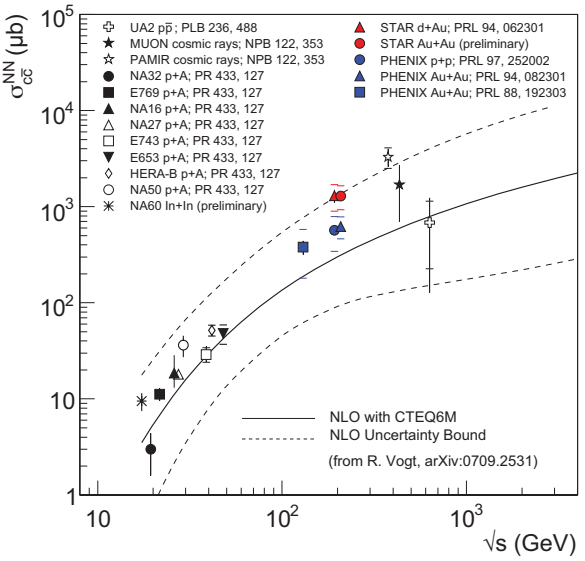

Figure 22: Comparison of total charm cross section measurements. The STAR and PHENIX results are given as cross section per binary collisions. Vertical lines reflect the statistical errors, horizontal bars indicate the systematic uncertainties (where available). From [162].

On the theory side, the state of the art for charm-quark production is NLO with the inclusion of $n_f = 3$ active flavors [132]. A few ingredients of the NNLO corrections are available [163, 164], but the full NNLO calculation has not been completed yet. Another possible approach to compute the cross section is to integrate the transverse momentum distribution computed in the so-called FONLL approximation, i.e. soft/collinear resummation to next-to-leading logarithmic accuracy (NLL), matched to the NLO result. The total cross section is still NLO, but the charm quark is treated as an active flavor, and therefore $n_f = 4$ in the calculation, which leads to a difference in the result [135].

The FONLL calculation can of course be employed to predict differential distributions, in particular the transverse momentum one, wherein contributions $\sim \alpha_S^k \ln^{k-2}(p_T/m_Q)$ (LL) and $\sim \alpha_S^k \ln^{k-3}(p_T/m_Q)$ (NLL), large for $p_T \gg m_Q$, are summed up to all orders. The spectra of c-flavored hadrons are then obtained by convoluting the charm distribution with the appropriate non perturbative fragmentation function, fitted, e.g., to LEP data. When doing the fit, the calculation of heavy-quark production in e^+e^- annihilation must be carried out in the same perturbative approximation, i.e. NLO+NLL, and the scales are to be consistently set [165, 166].

The main sources of uncertainty on such predictions

are the renormalization and factorization scales, the quark masses, entering in the perturbative calculation, parton distribution functions, such as the gluon density about the charm/bottom mass scale. As for the quark mass, it is also unclear whether in the calculation one should use the pole, the $\overline{\rm MS}$ or even the hadron mass. For the purpose of the PDFs, the gluon distribution exhibits large uncertainties at small x, especially a strong dependence on the factorization scale.

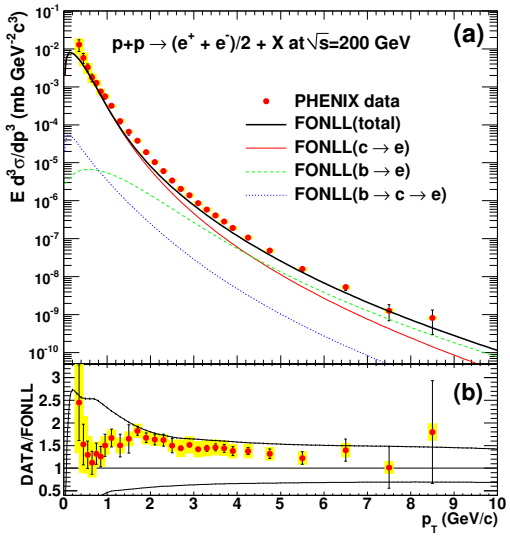

Figure 23: Non-photonic electron measurements at RHIC (PHENIX) in pp collisions at $\sqrt{s}$ = 200 GeV. (a) Invariant differential cross section of single electrons as a function of p_T. (b) The ratio of FONLL/Data as a function of p_T. The upper (lower) curve shows the theoretical upper (lower) limit of the FONLL calculation. From [158].

From the D- and B-hadron distribution one can derive the non-photonic electron spectrum at FONLL and compare it with RHIC data. Both the new PHENIX (shown in Fig. 23) and STAR pp data are compatible with the FONLL computation, within the theoretical and experimental uncertainties. However, the data favors large cross sections, about 1.5 times the nominal FONLL calculation, just on the upper edge of the uncertainty band (Fig. 23b). Non-photonic electron spectra at low p_T are notoriously difficult to analyze due to the increased photonic backgrounds, which increase the uncertainties for $p_T < 2$ GeV/c considerably and make the evaluation of $\sigma_{c\bar{c}}$ from electrons alone problematic.

Furthermore, much work has been carried out towards the separation of charm from bottom contributions to the lepton spectra in pp and pA collisions. Experimental progress has been made using e-h and e-D correlations [167, 168] shown in Fig. 24. Again, results

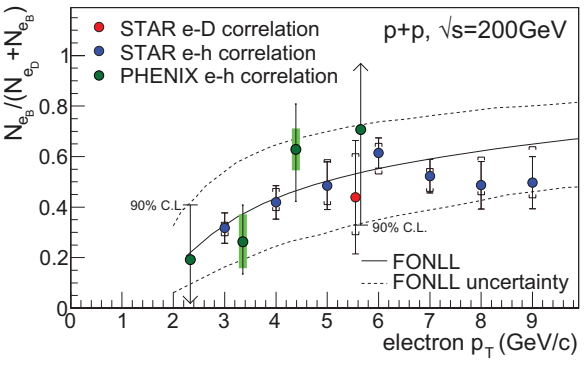

Figure 24: Transverse momentum dependence of the relative contribution from B mesons to the non-photonic electron yields as measured by PHENIX [167] and STAR [168]. Error bars are statistical and brackets/boxes are systematic uncertainties. The solid line is a FONLL prediction and the dotted lines represent the uncertainty on this FONLL prediction.

are consistent with the FONLL calculation, although experimental errors are currently still too large to allow an accurate separation of bottom and charm production in pp processes.

The final answer has to come from direct measurements of charm through D mesons (if able to subtract the $B \to D$ contribution looking e.g. at the impact parameter distribution) and that of bottom through $B \to J/\psi + X$ and/or b-tagged jets or leptonic decays. These measurements will require high precision vertexing that will become available for both RHIC experiments in the near future [162].

5.2. *Properties of gluon radiation off heavy quarks*

A heavy quark Q is characterized by the fact that its mass is much larger than the typical hadronization scale, say $m_Q \gg \Lambda_{\rm QCD}$, e.g., in the $\overline{\rm MS}$ renormalization scheme. The fact that the quark mass acts as a regulator of the collinear singularity and that the strong coupling constant is evaluated at relatively large scales, depending on the observable one is looking at, makes perturbative QCD applicable.

When dealing with multiple emissions from heavy quarks, an essential difference with respect to light quarks is that gluon radiation is suppressed inside the forward angular cone with an opening angle m_Q/E, the so-called dead cone, with E being the heavy-quark energy [169]. The dead cone implies the decrease of the overall energy loss and thus to the leading-particle effect, i.e. heavy-hadron energy distributions are peaked at large x, with x being the energy fraction in the centre-of-mass frame [136]. In other words, after multi-parton

radiation and hadronization, a heavy hadron still carries a significant fraction of the parent-quark energy. Also, for $x \simeq 1 - \Lambda_{\rm QCD}/m_Q$, one starts to be sensitive to non perturbative effects which can be included, e.g., by means of a fragmentation function or a frozen/effective coupling constant. Another relevant result, which can be related to the dead cone is that, unlike the naive parton-model expectation, the multiplicity difference between heavy and light hadrons is roughly independent of the centre-of-mass energy [170].

More generally, soft radiation obeys the Low–Barnett–Kroll (LBK) theorem [171, 172], according to which soft gluons are classical and therefore incapable of modifying the quantum numbers, such as the color, of a given system. Also, due to its classical nature, soft-parton emission is independent of the underlying hard-scattering process and of the quantum properties of the emitter. This implies that, if a process is forbidden by a given symmetry, such a veto cannot be relaxed by emitting extra soft photons/gluons.

This property of soft radiation can be connected to the longstanding puzzle of J/ψ production, whose measured rate at large p_T at the Tevatron was about 50 times larger than the theoretical prediction. In fact, the color-octet mechanism was formulated in order to explain such a discrepancy. In other words, such a model predicts, at one loop in gluon-gluon fusion, the production of a J/ψ and a gluon, with the J/ψ being in a color-octet state.

However, as discussed above, in order to change the J/ψ color, the emitted gluon cannot be soft: according to the LBK theorem, the price to pay for the emission of a hard gluon is $\sim (\Lambda_{\rm QCD}/m_c)^2$.

Therefore, it is probably worthwhile investigating alternative mechanisms which, besides the color-evaporation model and the color-octet model, can increase the yield of large-p_T J/ψ production in hadron collisions and hence recover the agreement with the Tevatron data. In fact, the production of quarkonia at large transverse momentum has a very small cross section and therefore it is a rare configuration, wherein fluctuations are expected to play a role [173].

5.3. Heavy quarks and energy loss in dense matter

A crucial issue in heavy-quark phenomenology is the description of energy loss in a dense medium and its relation to the quarkonium spectrum in matter. It is commonly assumed that partons at large transverse momentum traversing the medium lose energy through incoherent radiation of gluons as well as collisional energy loss. The approach presented in [174] assumes that a fast parton in a medium undergoes multiple collisions, characterized by a moderate momentum transfer and large values of the strong coupling constant. As for the coupling, non perturbative effects are taken into account by using a frozen coupling constant [136, 137]. Indeed, such a model manages to reproduce quite well the R_{AA} ratio measured by the PHENIX collaboration, for AuAu collisions at 200 GeV over the full transverse-momentum range, up to a normalization K-factor of about 2.

As for the radiative energy loss, for light quarks one usually relies on the Baier–Dokshitzer–Mueller–Peigné–Schiff (BDMPS) approximation [175] which assumes static scattering centres, independent soft emissions and hadronization outside the medium. For heavy quarks one can rely to the Gunion–Bertsch approach [176]: the medium-induced gluon-radiation spectrum is corrected by means of terms depending on the heavy-quark mass and on the fictitious gluon thermal mass. Moreover, gluons radiated by massive quarks are resolved in a smaller time with respect to light quarks, which implies a milder dependence on coherence effects and evolution variables for multiple radiation. Therefore, as a first approximation, one can even think of neglecting coherence effects when dealing with emissions from heavy quarks. The result is that if one adds both collisional and radiative energy loss contributions, a scaling factor of 0.6 is enough to reproduce the R_{AA} data at RHIC. Future data from the LHC will possibly shed light on the issue of the energy loss; to this goal, it will be very useful having more exclusive probes, such as azimuthal correlations or tagged c- or b-flavored jets. Another open issue concerns the gluon thermal mass and whether it can be theoretically predicted or it should rather be fitted to experimental data, like a non perturbative parameter.

5.4. Heavy quark plus photon production as a probe of the heavy quark PDF

The production of a direct photon accompanying a heavy quark at hadron colliders is an important process, also relevant to constrain the heavy-quark density. As it escapes confinement, a photon can be exploited to tag the hard scattering; also, its transverse momentum distribution gives meaningful information on the heavy-quark production process and PDF.

At leading order, i.e. $O(\alpha\alpha_S)$, there is only one hard scattering process, namely $gQ \to Q\gamma$. At NLO in the strong coupling constant, i.e. $O(\alpha\alpha_S^2)$, several subprocesses contribute to $Q\gamma$ production, with gluons, heavy and light quarks in the initial state [177]. Considering, e.g., charm production, such processes will help to shed light on the charm distribution and whether it is radiatively generated by means of gluon emissions, in which

case $c(x, Q^2) \simeq g(x, Q^2)$, or there is an intrinsic charm contribution to the proton. In fact, there exist light cone models, wherein intrinsic charm is relevant at large x [178], and sea-like models, with $\bar{c}(x) \simeq \bar{u}(x) + \bar{d}(x)$. As for the comparison between the photon spectra produced in association with charm and bottom quarks, there are remarkable differences both at LO and at NLO. At large transverse momenta, the discrepancy between LO and NLO gets larger [177].

The NLO calculation has been compared with D0 data [179] on the photon transverse momentum in $Q\gamma$ events: the agreement is pretty good in the case of $b\gamma$ production, whereas discrepancies are present for charm production, with the NLO computation yielding a lower cross section for moderate and large values of p_T. Such disagreement can be traced back to the possible existence of intrinsic charm in the proton. Using the Brodsky–Hoyer–Peterson–Sakai (BHPS) PDF set [178] slightly improves the comparison, although meaningful differences are still present at very large p_T. The discrepancy is instead milder when comparing the ratio of charm and bottom cross sections. At the LHC, one can still investigate the presence of the intrinsic charm. However, since the probed values of x are on average smaller than at the Tevatron, one is basically sensitive to the sea-like model. Also, the forward-rapidity region will be particularly suitable to discriminate between radiative and intrinsic contributions to the charm PDF.

The LO/NLO calculations for $b/c + \gamma$ production can be extended to pA collisions, e.g. proton-lead processes at the LHC. A first approximation consists in using the same amplitudes as in the vacuum and convoluting them with nuclear parton densities, such as the EPS [55], HKN [180] and nCTEQ [181] sets. Unlike the proton case, the gluon distribution in a nucleus is poorly known, and it is one of the main differences among the nuclear PDF sets. In fact, possible measurements at the LHC of $\gamma + c/b$ final states will help to investigate both gluon and charm/bottom distributions in dense matter.

Likewise, similar studies can be carried out for deuterium-gold collisions at RHIC. Since the Bjorken-x regions probed at RHIC and LHC are complementary, these measurements will help to discriminate among the nuclear parton distribution sets. As for the hard scattering, how to implement medium modifications, for both light and heavy quark production, is still an open issue; moreover, collinear factorization is an assumption that has not yet been proved. The BDMPS and Gunion–Bertsch approximations discussed above work well only for soft/collinear emissions. Indeed, there are prescriptions for hard/large-angle radiation, but a thorough implementation and phenomenological analysis on medium-modified hard scatterings is still missing. Convoluting possible medium-induced hard matrix elements with nuclear parton densities will ultimately lead to cross sections fully including dense-matter effects.

6. Quarkonia as a Tool

6.1. Proton-Proton Collision Studies

Since the start of LHC operation, new experimental data on quarkonium production has revived the interest in understanding the production mechanisms of various quarkonium states in hadronic collisions. All the models describing various sources of onia in hadronic collisions share the common basis: the factorisation between the hard collison subprocess and the parton-parton collision luminosity, calculated as a convolution of the parton distribution functions (PDFs).

Clearly, the range of accessible $x_{1,2}$ depends on the rapidity interval covered by the experiments. For charmonium at the Tevatron, with a partonic center-of-mass energy $\sqrt{\hat{s}} \simeq 3.5$ GeV, $\sqrt{s} \simeq 2$ TeV, the CDF range is :

$$y \simeq 0 \quad \Rightarrow \quad x_{1,2} \simeq 1.8 \times 10^{-3}$$

while for D0:

$$-1.6 \lesssim y \lesssim 1.6 \quad \Rightarrow \quad x_{1,2} \simeq (0.36 - 8.9) \times 10^{-3}$$

Their values of $x_{1,2}$ lie within the range where the PDFs are well-established. Hence the uncertainties on the parton luminosities at the Tevatron are fairly small.

At the LHC, not only is the energy higher by a factor of 3.5, but the rapidity coverage of the various experiments is also significantly wider, especially if one combines the results from ATLAS and CMS with those of LHCb and ALICE. One get for ATLAS and CMS:

$$-2.4 \lesssim y \lesssim 2.4 \quad \Rightarrow \quad x_1 \simeq (0.04 - 6.0) \times 10^{-3}$$
$$x_2 \simeq (6.0 - 0.04) \times 10^{-3}$$

while for LHCb:

$$2 \lesssim y \lesssim 5 \quad \Rightarrow \quad x_1 \simeq (4 - 80) \cdot 10^{-3}$$
$$x_2 \simeq (0.07 - 0.003) \times 10^{-3}$$

ALICE has complementary coverages ($|y| < 1$ & $2.5. < y < 4.0$). For the kinematics of LHC experiments, the accessible x range of charmonium production measurements is up to three orders of magnitude below the "safe" value of 10^{-3}. Processes usually used for determining gluon PDFs, such as jets, prompt photons or open charm pairs, are for various reasons unlikely to be useful at these extremely low x, leaving charmonium as

the only source of information on gluon PDFs in this area.

The smallest $\sqrt{\hat{s}}$ value for bottomonium is about 10 GeV, three times larger than for charmonium. This restricts the "reach" of Υ studies to $x_{1,2}$ values three times larger than those contributing to J/ψ. However, this is still significantly smaller than the currently accessible range, and thus should be useful as a consistency check and maybe also to test the Q^2 evolution (providing data with a higher Q^2 for similar x_B, which may be helpful to differentiate between a BFKL- and DGLAP-like evolution).

The main experimental difficulties include a reduced acceptance for J/ψ when both p_T and $|y|$ are small, and the necessity of suppressing non-prompt charmonia (which come from larger $\hat{s}$). Theoretical complications include proper and consistent treatment of intrinsic parton p_T, initial-state radiation, and higher-order perturbative effects, as well as the possibility of gluon recombination at high densities. So concerted efforts from theorists and experimentalists will be needed to extend our measurements of the PDFs to much smaller x than prior to the LHC. This is necessary for understanding the dynamics of quarkonium hadronic production.

6.2. Nuclear Collision Studies

From statistical QCD we know that strongly interacting matter undergoes a deconfinement transition to a new state, the quark-gluon plasma (QGP). The objective of high energy nuclear collisions is to produce and study the QGP under controlled conditions in the laboratory. How then can we probe the QGP - what phenomena provide us with information about its thermodynamic state? Here the ultimate aim must be to carry out *ab initio* calculations of the in-medium behaviour of the probe in finite temperature QCD. Quarkonia may well provide the best tool for this presently known, but in nuclear collisions other phenomena will also lead to modified quarkonium production. As a consequence, parton distribution changes, parton energy loss and cold nuclear matter effects (absorption) on quarkonium production must be accounted for before any QGP studies become meaningful. For the sake of definiteness, in this section we shall refer to the non-QGP effects as normal, in contrast to the anomalous suppression (or enhancement) we want to look for.

Any modifications observed when comparing J/ψ production in AA collisions to that in pp interactions thus have two distinct origins. Of primary interest is obviously the effect of the secondary medium produced in the collision - this is the candidate for the QGP we want to study. In addition, however, the presence of the "normal" initial and final state effects will presumably also affect the production process and the measured rates. This ambiguity in the origin of any observed J/ψ suppression will thus have to be resolved.

A second empirical feature to be noted is that the observed J/ψ production consists of directly produced $1S$ states as well as of decay products from χ_c(1P) and ψ'(2S) production. The presence of a hot QGP affects the higher excited quarkonium states much sooner (at lower temperatures) than the ground states. This results in another ambiguity in observed J/ψ production - are only the higher excited states affected, or do all states suffer?

An ideal solution of these problems would be to measure separately J/ψ, χ_c and ψ' production first in pA (or dA) collisions, to determine the effects of cold nuclear matter, and then measure, again separately, the production of the different states in AA collisions as function of centrality at different collision energies.

Until such studies become available, we resort to a more operational approach, whose basic features are:

- We assume that the J/ψ feed-down rates in pA and AA are the same as in pp, i.e., 60 % direct J/ψ , 30 % decay of $\chi(1P)$, and 10 % decay of $\psi'(2S)$.
- We specify the effects due to cold nuclear matter by a Glauber analysis of pA or dA experiments in terms of $\sigma^i_{\rm abs}$ for $i = J/\psi, \chi_c, \psi'$. This $\sigma^i_{\rm abs}$ is not meant to be a real cross section for charmonium absorption by nucleons in a nucleus; it is rather used to parametrize all initial and final state nuclear effects, including shadowing/antishadowing, parton energy loss and pre-resonance/resonance absorption.
- In the analysis of AA collisions, we then use $\sigma^i_{\rm abs}$ in a Glauber analysis to obtain the predicted form of *normal* J/ψ suppression. This allows us to identify *anomalous* J/ψ suppression as the difference between the observed production distribution and that expected from only normal suppression. We parametrize the anomalous suppression through the survival probability

$$S_i = \frac{(dN_i/dy)_{\rm exp}}{(dN_i/dy)_{\rm Glauber}} \qquad (14)$$

  for each quarkonium state i.

With the effects of cold nuclear matter thus accounted for, what form do we expect for anomalous J/ψ suppression? If AA collisions indeed produce a fully equilibrated QGP, we should observe a sequential suppression pattern for J/ψ and Υ, with thresholds predicted

(quantitatively in temperature or energy density) by finite temperature QCD [183, 184, 185, 186]. The resulting pattern for the J/ψ is illustrated in Fig. 25.

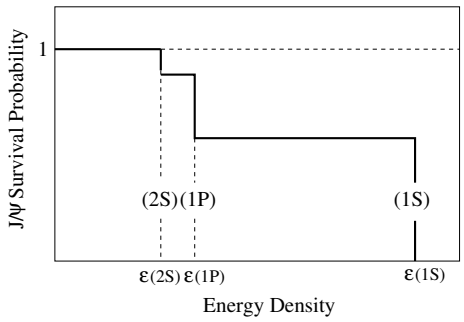

Figure 25: Illustration of sequential J/ψ suppression.

Its consequences are quite clear. If, as present statistical QCD studies indicate, the direct J/ψ survives up to about 2 T_c and hence to $\epsilon \geq 25$ GeV/fm^3, then all anomalous suppression observed at SPS and RHIC must be due to the dissociation of the higher excited states χ_c and ψ'. The suppression onset for these is predicted to lie around $\epsilon \simeq 1$ GeV/fm^3, and once they are gone, only the unaffected J/ψ production remains. Hence the J/ψ survival probability for central AuAu collisions at RHIC should be the same as for central PbPb collisions at the SPS.

A further check to verify that the observed J/ψ production in central collisions is indeed due to the unmodified survival of the directly produced $1S$ state is provided by its transverse momentum behaviour. Initial state parton scattering causes a broadening of the p_T distributions of charmonia [187, 188, 189]: the gluon from the proton projectile in pA collisions can scatter a number of times in the target nucleus before fusing with a target gluon to produce a $c\bar{c}$. Assuming the gluon from the proton to undergo a random walk through the target leads to

$$\langle p_T^2 \rangle_{pA} = \langle p_T^2 \rangle_{pp} + N_c^A \delta_0 \qquad (15)$$

for the average squared transverse momentum of the observed J/ψ. Here N_c^A specifies the number of collisions of the gluon before the parton fusion to $c\bar{c}$, and δ_0 the kick it receives at each collision. The collision number N_c^A can be calculated in the Glauber formalism; here $\sigma_{\rm abs}$ has to be included to take the presence of cold nuclear matter into account, which through a reduction of J/ψ production shifts the effective fusion point further "down-stream" [190].

In AA collisions, initial state parton scattering occurs in both target and projectile and the corresponding random walk form becomes

$$\langle p_T^2 \rangle_{AA} = \langle p_T^2 \rangle_{pp} + N_c^{AA} \delta_0, \qquad (16)$$

where now N_c^{AA} denotes the sum of the number of collisions in the target and the projectile prior to parton fusion. It can again be calculated in the Glauber scheme including $\sigma_{\rm abs}$. The crucial point now is that if the observed J/ψ's in central AA collisions are due to undisturbed $1S$ production, then the centrality dependence of the p_T broadening is fully predicted by such initial state parton scattering [186]. In contrast, any onset of anomalous suppression of the J/ψ would lead to a modification of the random walk form [190].

In Fig. 26 we summarize the predictions for J/ψ survival and transverse momentum behaviour in AA collisions at SPS and RHIC, as they emerge from our present state of knowledge of statistical QCD. Included are some preliminary and some final data; for a discussion of the data analysis and selection, see Ref. [186].

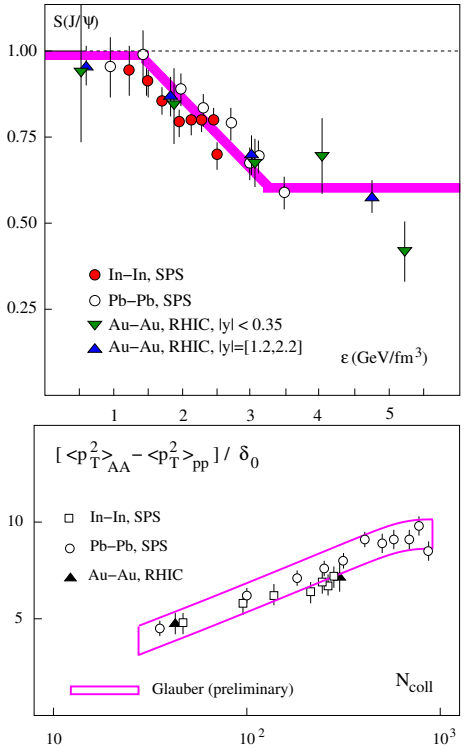

Figure 26: J/ψ survival and transverse momentum at SPS and RHIC.

We conclude that the present experimental results are compatible with the present information from statistical QCD. This was not the case previously, and such a conclusion can be drawn today because of several changes in our theoretical and experimental understanding.

- Finite T lattice QCD suggests direct J/ψ suppression at energy densities beyond the RHIC range; previous onset values were much lower (see, e.g., Ref. [182]).
- SPS InIn data suggest an onset of anomalous suppression at $\epsilon \simeq 1$ GeV/fm^3; previous onset values from PbPb and SU interactions were considerably higher, with $\epsilon \simeq 2 - 2.5$ GeV/fm^3 (see, e.g., Ref. [191]).
- Within statistics, there is no further drop of the J/ψ survival rate below 50 - 60 %, neither at RHIC nor at the SPS; a second drop in very central SPS PbPb data (see, e.g., Ref. [191]) is no longer considered viable.

6.2.1. J/ψ Enhancement by Regeneration

In this section we want to consider an alternative approach which can so far also account for the available data. The basic idea here is that the medium produced in nuclear collisions is not a QGP in full equilibrium but rather one which is oversaturated in its charm content.

A crucial aspect in the QGP argumentation of the previous sections was that charmonia, once dissociated, cannot be recreated at the hadronization stage since the abundance of charm quarks in an equilibrium QGP is far too low to allow this. The thermal charm quark production rate, relative to that of light quarks, is

$$\frac{c\bar{c}}{q\bar{q}} \simeq \exp\{-m_c/T_c\} \simeq 6 \times 10^{-4}, \qquad (17)$$

with $m_c = 1.3$ GeV for the charm quark mass and $T_c = 0.175$ GeV for the transition temperature. The initial charm production in high energy nuclear interactions, however, is a hard non-thermal process, and the resulting $c/\bar{c}$ production rates grow with the number ($N_{\rm coll}$) of nucleon-nucleon collisions. In contrast, the light quark production rate grows (at least in the present energy regime) essentially as the number ($N_{\rm part}$) of participant nucleons, i.e., much slower. The initial charm abundance in AA collisions is thus much higher than the thermal value; we illustrate this in Fig. 27 for $A = 200$ as function of the collision energy $\sqrt{s}$. What happens to this excess in the course of the collision evolution?

The basic assumption of the regeneration approach [192, 193, 194] is that the initial charm excess is maintained throughout the subsequent evolution, i.e., that the initial chemical non equilibrium will persist up to the hadronization point. If that is the case, a c from a given nucleon-nucleon collision can, at hadronization, combine with a $\bar{c}$ from a different collision ("off-diagonal" pairs) to recreate a J/ψ. This pairing provides a new secondary statistical charmonium production mechanism,

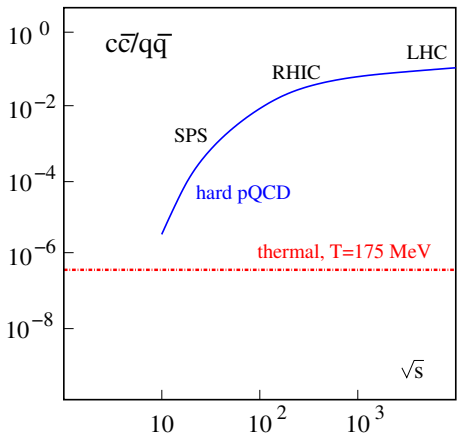

Figure 27: Thermal vs. hard charm production.

in which the c and the $\bar{c}$ in a charmonium state have different parents, in contrast to the primary dynamical production in a pp collision. At sufficiently high energy, this mechanism will lead to enhanced J/ψ production in AA collisions in comparison to the scaled pp rates. When should this enhancement set in?

In recent work [192, 193, 194], it is generally assumed that the direct J/ψ production is strongly suppressed for $\epsilon \geq 3$ GeV/fm^3. This is evidently in contrast to the statistical QCD results discussed in the previous sections; however, we recall the caveat that the temperature dependence of the charmonium widths is so far not known. Moreover, it is of course always possible that the medium produced in nuclear collisions is quite different from the quark-gluon plasma of statistical QCD.

Next, it is assumed that the regeneration rate is determined by statistical combination in a QGP in *kinetic* equilibrium, with or without wave function corrections. In other words, if a c and a $\bar{c}$ meet under the right kinematic conditions, they are taken to form a J/ψ. An evolution towards a QGP in *chemical* equilibrium would also allow annihilation at this point.

To account for the J/ψ production rates observed at RHIC, it is then assumed that the new statistical production just compensates the proposed decrease of the direct primary $1S$ production, as illustrated in Fig. 28. At the LHC, with much higher energy densities, one should then observe a J/ψ enhancement relative to the rates expected from scaled pp results.

We thus have to find ways of distinguishing between the two scenarios discussed here: the sequential suppression predicted by an equilibrium QGP or a stronger direct suppression followed by a J/ψ regeneration in a medium with excess charm. Fortunately the basic production patterns in the two cases are very different, so

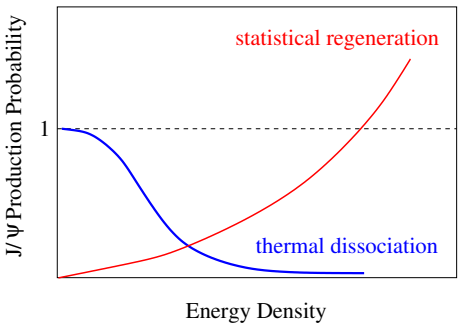

Figure 28: Illustration of regeneration of J/ψ production.

that one may hope for an eventual resolution.

The overall J/ψ survival probability in the two cases is illustrated in Fig. 29. Sequential suppression provides a step-wise reduction: first the higher excited charmonium states are dissociated and thus their feed-down contribution disappears; at much higher temperature, the J/ψ itself is suppressed. Both onsets are in principle predicted by lattice QCD calculations. In the regeneration scenario, the thermal dissociation of all "diagonal" J/ψ production is obtained by extrapolating SPS data to higher energy densities. The main prediction of the approach is therefore the increase of J/ψ production with increasing energy density. Ideally, the predictions for the LHC are opposite extremes, providing of course that here the feed-down from B-decay is properly accounted for.

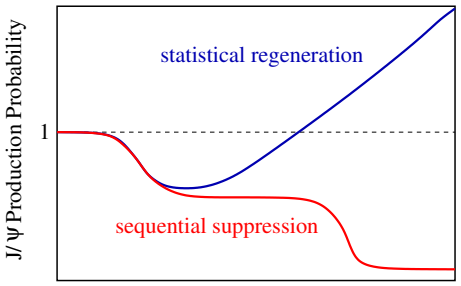

Figure 29: J/ψ survival: sequential suppression vs. regeneration.

The expected transverse momentum behaviour in the two cases is also quite different. In the region of full J/ψ survival, sequential suppression predicts the normal random walk pattern specified through pA studies; the eventual dissociation of direct J/ψ states then leads to an anomalous suppression also in the average p_T^2 [190]. Regeneration alone basically removes the centrality dependence since the different partners come from different collisions. It is possible to introduce some small centrality dependence [195], but the random walk increase is essentially removed. The resulting behaviour is schematically illustrated in Fig. 30. More generally, the quarkonium momentum distributions, whether transverse or longitudinal, should in the regeneration scenario be simply a convolution of the corresponding open charm distributions; this provides a further check [195].

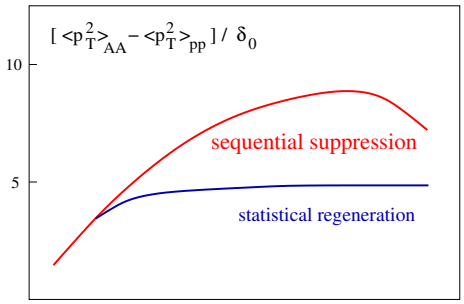

Figure 30: p_T-behaviour: sequential suppression vs. regeneration.

6.2.2. *Conclusions*

- In statistical QCD, the spectral analysis of quarkonia provides a well-defined way to determine temperature and energy density of the QGP.
- If nuclear collisions produce a quark-gluon plasma in equilibrium, the study of quarkonium production can provide a direct way to connect experiment and statistical QCD.
- For a QGP with surviving charm excess, off-diagonal quarkonium formation by statistical combination may destroy this connection and instead result in enhanced J/ψ production.

7. New observables in quarkonium production

In order to better understand the mechanisms responsible for heavy quarkonium production, it is now essential to introduce new observables. The theoretical uncertainties on the predicted yields are too large to draw any strong conclusions on production models. Moreover, polarization studies are known to be experimentally challenging and not always possible over the full phase-space region even if the yield is otherwise measured. The LHC will certainly provide new information on the yields and polarizations. In addition, the LHC is well positioned to make unique new measurements

previously unavailable due to unsufficient luminosity, center-of-mass energy, detector resolution or even manpower.

7.1. Hadronic activity around quarkonium

The first observable that we discuss, hadronic activity around quarkonium [196], is, in fact, not completely new. Indeed, UA1 compared their charged-track distributions with Monte Carlo simulations of a J/ψ coming from a B decay and a J/ψ coming from a χ_c decay [197, 198]. In the early nineties –before the Tevatron results– χ_c feed-down was still expected to be the major source of prompt J/ψ production. However, if we assume either that production proceeds through CO transitions or through CS transitions at higher-orders, we now expect more complex distributions, even for the prompt yield. It is therefore not clear how accurately such methods – recently revived by STAR in [13] – can determine the B-feeddown to J/ψ, other than with measurements of displaced vertices typical of B decays. Instead, the hadronic activity around quarkonium could be a good discriminant between CO and CS contributions to quarkonium production since gluon emission during CO transitions would increase the hadronic activity. This study is, however, difficult to carry out in practice [196].

7.2. Associated production

We therefore urgently need more observables easier to predict that test the many production models available [107, 109]. We argue that the study of associated production channels, $\psi + c\bar{c}$ and $\Upsilon + b\bar{b}$, first in pp collisions, then in pA and AA, fills both these requirements. These reactions are potentially very interesting since the LO description already shows leading p_T behaviour. We expect that higher-QCD corrections will be less important and the cross section will thus be less sensitive to the renormalisation scale, allowing for more precise predictions.

Further motivation for such studies is the amazingly large fraction of J/ψ produced in association with another $c\bar{c}$ pair at B-factories. For instance, the Belle collaboration first found [199]

$$\frac{\sigma\,(e^+e^- \to J/\psi + c\bar{c})}{\sigma\,(e^+e^- \to J/\psi + X)} = 0.59^{-0.13}_{+0.15} \pm 0.12. \qquad (18)$$

More recently, the Belle collaboration reported new measurements [37]:

$$\begin{aligned} \sigma\,(J/\psi + X) &= 1.17 \pm 0.02 \pm 0.07 \text{ pb}\,, \\ \sigma\,(J/\psi + c\bar{c}) &= 0.74 \pm 0.08^{+0.09}_{-0.08} \text{ pb}\,, \\ \sigma\,(J/\psi + X_{\text{non } c\bar{c}}) &= 0.43 \pm 0.09 \pm 0.09)\text{ pb}, \end{aligned} \qquad (19)$$

which confirm that associated $J/\psi + c\bar{c}$ production is the dominant production mechanism at B factories.

Until now, it is unknown whether such a high associated fraction also holds for hadroproduction. Analyses at the Tevatron (CDF and $D0$) and at RHIC (PHENIX and STAR) are feasible, in addition to the LHC. The predicted Tevatron Run II integrated cross sections at $\sqrt{s} = 1.96$ TeV are significant [23] :

$$\begin{aligned} \sigma(J/\psi + c\bar{c}) \times Br(\ell^+\ell^-) &\simeq 1 \text{ nb}, \\ \sigma(\Upsilon + b\bar{b}) \times Br(\ell^+\ell^-) &\simeq 1 \text{ pb}. \end{aligned} \qquad (20)$$

Neglecting the likely reduction of the CO matrix elements needed to comply with the e^+e^- results and induced by higher-order QCD corrections to the color-singlet contributions (see section 2), the integrated cross sections for associated $J/\psi + c\bar{c}$ production were found [200] to be dominated by the CS part. This is also the case for the p_T distribution up to at least 5 GeV for ψ and 10 GeV for Υ. This clearly means that such observables directly probe the CS mechanism. For most of the other observables, it is not as clear whether the CO contribution dominante over the CS one and they cannot be regarderd as a clean probe of CS constributions due to the inherent uncertainty from the CO yield.

If the effect of CO transitions is indeed negligible for *inclusive* Υ production, Υ's produced in association with a $b\bar{b}$ pair would be unpolarised at the LHC, independent of p_T.

Besides discriminating between the CO and the CS transitions, the ψ yield in association with a $c\bar{c}$ should show an *a priori* completely different sensitivity to the χ_c feed-down than the inclusive yield. The same holds true for $\Upsilon + b\bar{b}$ relative to χ_b feed-down. The CS P-state yield is expected to be smaller than the S-state one since they are suppressed by powers of the relative velocity v. Contrary to the inclusive case, no additional gluon is needed to attach to the heavy quark loop to produce the ψ (or Υ) compared to P-states.

For the CO transitions, associated production of $\chi_c + c\bar{c}$ can occur via $gg \to gg$ where both final-state gluons split into $c\bar{c}$ pairs. One of them then hadronizes into a χ_c via a CO transitions. This contribution is certainly suppressed up to $p_T \simeq 20$ GeV. At larger p_T, a dedicated calculation is needed. However, this mechanism could be easily disentangled from the CS contributions since both c quarks are necessarily emitted back to back from the χ_c and thus to the J/ψ.

The non-prompt signal would originate as usual from $gg \to b\bar{b}$, where one b quark decays into a $\psi + X$. Usually, hadronisation of the b produces the ψ with light

quarks only. This means that we have a single c quark in the event, produced from the decay of the recoiling b quark and therefore back to back from the ψ. The non-prompt signal could then be simply suppressed down by searching for a D meson near the ψ. It is possible that hadronisation of the b produces both the ψ and a D meson. In this case, kinematic cuts would not help suppress the non-prompt yield. Fortunately, this final state is *a priori* suppressed compared to the first case and even further suppressed relative to the direct yield. Indeed, there is no gain in the p_T dependence since both the $gg \to b\bar{b}$ and $gg \to \psi + c\bar{c}$ cross sections scale like p_T^{-4}. A cross check sizing up the non-prompt yield with a displaced vertex measurement would be instructive.

Associated production has also been studied in direct $\gamma\gamma$ collisions in ultraperipheral collisions (UPC) [201]. At least for direct $\gamma\gamma$ collisions, associated production is the dominant contribution to the inclusive rate for $p_T \geq 2$ GeV/c.

To conclude, studies can be carried on by detecting either the "near" or "away" heavy-quark with respect to the quarkonia. There are, of course, different ways to detect the D, B, or b-jet, ranging from a displaced vertices to detection of semileptonic decays to e or μ.

As mentionned in section 4, associated production of J/ψ or Υ with a prompt photon may also be investigated at the LHC. Interestingly, contrary to the inclusive case, the $C = +1$ CO should impact the large p_T region, while $C = -1$ CO the small and mid p_T region. The NLO CS contribution was recently studied [127] and, contrary to the inclusive case, it was shown that for this process the CO and CS induced yield should be similar, even with the largest possible CO matrix elements. At NNLO, the CS yield is expected to be further enhanced [128] and to dominate over the CO yield. The measurements of J/ψ and Υ production associated with a direct photon at hadron colliders could thus be an important test of the theoretical treatment of heavy-quarkonium production.

The background to these processes should also be taken into account. The Quarkonium event generator Madonia [202], imbedded in Madgraph [203], will surely be of a great help in achieving this. In any case, we hope that such measurements would provide clear information on the mechanisms at work in quarkonium production.

8. Conclusion

Quarkonium production measurements in pp collisions have motivated many theoretical investigations. However, despite advances, there is still no clear picture of the quarkonium hadroproduction mechanism. Such a mechanism should be able to explain both the cross section and the polarization measurements at the Tevatron and RHIC, as well as comparable measurements at B factories and lepton-hadron colliders. Presently, we have several different approaches at our disposal, such as the Color Singlet Model (CSM), in which the $Q\bar{Q}$ is produced color neutral at short distances, and Non-Relativistic QCD (NRQCD), where quarkonium production can also proceed via creation of color-octet $Q\bar{Q}$ pairs, via the Color Octet Mechanism (COM). These approaches have both advantages and disadvantages.

NRQCD has successfully explained the excess in charmonium production reported by the CDF Collaboration, orders of magnitude larger than the LO CSM. However so far it fails to provide a consistent description of production and polarization in pp collisions and the rates at B factories.

Higher order corrections in α_s have only recently been calculated. The CS corrections at high p_T are very large given that the corrections open new production channels which are relevant at high p_T. On the contrary, CO calculations show that the cross sections do not increase much when these corrections are taken into account since NLO CO contributions do not open any new channels. The contributions of the NLO CS corrections reduce the discrepancy between the CSM cross sections and the CDF data, but still fall too steeply at high p_T to describe this region successfully. The NNLO* contribution may be able to fill the gap between calculations and high p_T data. At RHIC, the high p_T STAR data seems to favor the COM over the CSM, while at low p_T the PHENIX data are well reproduced by both approaches. It is, however, worth noting that little is known about feed down contributions at RHIC, while there does not exist any NLO theoretical predictions for the χ_c yield, in either approach.

In addition, the LO NRQCD calculation predicts a sizable transverse polarization rate for large p_T J/ψ whereas the Tevatron CDF measurement at Fermilab displays a slight longitudinal polarization at large p_T for the prompt yield. This problem is still present in calculations at NLO, since these corrections only slightly change the p_T dependence of J/ψ production rate and polarization with respect to the LO calculations. However, the CSM results drastically change from transverse-polarization dominance at LO to longitudinal-polarization dominance at NLO, nearly in agreement with the data on J/ψ polarization produced in pp collisions both at the Tevatron and RHIC, if the polarization of the J/ψ from χ_c feed down is assumed.

In order to solve this puzzle, improved measurements are needed. So far, most experiments have presented

results based on a fraction of the physical information derivable from the data: only one polarization frame is used and only the polar projection of the decay angular distribution is studied. These incomplete results prevent model-independent physical conclusions. In the forthcoming LHC measurements, it is important to approach the polarization measurement as a multidimensional problem, determining the full angular distribution in more than one frame.

The feed downs from more massive states, such as higher-mass quarkonium states, cannot yet be taken into account in most of the calculations. While there are CDF measurements of direct production, the χ_c feed down can significantly influence the polarization of the prompt J/ψ yield. A better way to avoid the feed-down problem is to study ψ' and $\Upsilon(3S)$ where no important feed down from higher excited states exist.

The behavior of quarkonium production in pA collisions due to Cold Nuclear Matter (CNM) effects is not yet understood. Puzzling features in proton-nucleus data put forward new aspects of charmonium physics in nuclear reactions, namely the role of cold nuclear matter effects (CNM). Two CNM effects are considered to be of particular importance: the modification of the initial parton distributions (PDFs) due to the nuclear environment, an initial-state effect known as shadowing; and the breakup of $c\bar{c}$ pairs after multiple scatterings with the remnants of target nucleus, referred to as the nuclear absorption.

Parton shadowing in the target nucleus may suppress (or enhance, in case of antishadowing) the probability of producing a J/ψ. Its effect depends on the kinematics of the $c\bar{c}$ pair production. The theoretical expectations for gluon shadowing are quite diverse. A weak shadowing effect was predicted by the dipole approach and in some analysis of DIS data such as the one developed by deFlorian and Sassot at leading and next-to-leading order – the nDS and nDSg parameterizations –. However, strong gluon shadowing and antishadowing was obtained in the EKS98, EPS08, and EPS09 parameterizations by Eskola and collaborators. We note that some pA data were included in the EPS08 and EPS09 analyses. The nDSg and EKS98 parameterizations are compatible for $x < 10^{-3}$.

Secondly, there is the effect of the nuclear absorption. The strength of the interaction of the evolving $c\bar{c}$ pair with the target nucleons can break up the pair and consequently suppress the J/ψ yield. The intensity of this effect may also depend on the quantum states of the $c\bar{c}$ pair at the production level (color octet or color singlet), and on the kinematic variables of the pair. Indeed, a colorless $c\bar{c}$ pair created in a hard reaction is not yet charmonium since it does not have a fixed mass. It takes time to disentangle ground state charmonium from its excitations, $t_f \sim 1/(m^2_{\psi'} - m^2_{J/\psi})$. This time scale is interpreted as the formation time of the charmonium wave function. At low energies, this time is shorter than the mean nucleon spacing in a nucleus so that the formation process can be treated as instantaneous. At much higher energies, the formation time is long and the initial size of the $c\bar{c}$ dipole is "frozen" by Lorentz time dilation while propagating through the nucleus.

According to the above arguments, at high energy, the heavy state in the projectile should undergo coherent scattering off the nucleons of the target nucleus, in contrast to the incoherent, longitudinally ordered scattering that takes place at low energies. This should lead to a decrease of $\sigma^{\rm abs}_{J/\psi}$ with increasing energy $\sqrt{s_{NN}}$. Compilation and systematic study of many experimental data indicate that $\sigma^{\rm abs}_{J/\psi}$ appears either constant or decreasing with energy, following the most recent theoretical expectations.

The energy regime recently opened up by the advent of the LHC offers new possibilities. Clearly pA data at the LHC are essential to investigate various physics effects, in particular nuclear shadowing in a still unexplored x-range. The final-state interaction of quarkonia with CNM is another attractive topic. Due to the expected very short overlap time of the heavy-quark pair with nuclear matter, one could expect its influence on the still almost point-like $c\bar{c}$ to be rather limited. However, these considerations are still very qualitative and deeper theoretical studies are clearly necessary.

The study of open heavy flavour production in pp and pA collisions is tightly connected to the process of quarkonia (hidden flavor) production. It offers a good basis to establish fundamental parameters for quarkonium calculations, together with an outstanding framework to test fundamental concepts, such as perturbative QCD, factorization and non-perturbative power corrections. Because heavy quarks are massive, the production cross section can be calculated in perturbative QCD down to $p_T = 0$ at the parton level.

However, differential distributions and event shapes exhibit large logarithmic contributions, typically corresponding to soft or collinear parton radiation, which need to be resummed to all orders. Furthermore, dead-cone effects suppress gluon radiation around the heavy-quark direction, which has relevant phenomenological implications on both parton- and hadron-level spectra. As far as heavy-hadron production is concerned, one can model non perturbative effects by means of hadronization models such as the Lund-based string models, which are implemented within the frame-

work of Monte Carlo generators HERWIG, PYTHIA, MC@NLO, etc. Multi-purpose generators have been available for several years for lepton/hadron collisions in the vacuum and some have been lately modified to include the effects of dense matter.

In order to promote the formalism used to describe open heavy flavors to pA and ultimately AA collisions, one has to introduce medium-modification effects. In particular, one of the most striking observations of heavy-ion collisions is the jet-quenching phenomenon, namely the suppression of hadron multiplicity at large transverse momentum with respect to pp processes. In the case of heavy hadrons, the measured suppression is expected to be lower than that of light-flavor mesons, due to the dead-cone effect. So far, suppression of heavy-flavored mesons in pA or AA collisions has only been measured through leptons (non-photonic electrons and single muons), i.e., the leptons from semi leptonic decays of heavy-flavored hadrons. Surprisingly, the energy loss observed through heavy-flavor leptons is substantial already at moderate p_T of ~3 GeV/c. Several mechanisms to describe heavy-flavor energy loss in the dense medium have been proposed. Most prominent are collisional and radiative energy loss, typically calculated in the weak-coupling regime. However, the magnitude of the observed suppression at RHIC is hard to accommodate in these models. Recent attempts, assuming strong coupling between the heavy-flavor mesons and the dense medium and based on AdS/CFT correspondence lead to higher suppression factors. Further studies as well as experimental data are needed before any conclusions can be drawn. Future data from the LHC will possibly shed light on the issue of the energy loss. It will be very useful to have more exclusive probes such as azimuthal correlations or tagged c- or b-flavored jets.

Another crucial issue in heavy-flavor phenomenology concerns heavy-quark parton distributions in protons and nuclei. In fact, processes with the production of heavy quarks are fundamental to constrain the PDFs. In particular, the production of a direct photon accompanying a heavy quark at hadron colliders is an important process, also relevant to constrain the heavy-quark density. As it escapes confinement, a photon can be exploited to tag the hard scattering; also, its transverse momentum distribution gives meaningful information on the heavy-quark production process and PDF.

The LO/NLO calculations for $\gamma + c/b$ production can be extended to pA collisions, e.g. proton-lead processes at the LHC. To a first approximation, the process can be calculated by convoluting the vacuum matrix elements with nuclear PDFs. While the gluon distribution in the proton is rather well constrained, it is poorly known in the nucleus, hence large discrepancy between gluon shadowing parametrizations. In fact, possible measurements at the LHC of $\gamma + c/b$ final states will help to investigate both gluon and charm/bottom distributions in dense matter. Since the Bjorken-x regions probed at RHIC and LHC are complementary, these measurements will help to discriminate among the nuclear parton distribution sets.

Lattice QCD calculations predict that, at sufficiently large energy densities, hadronic matter undergoes a phase transition to a plasma of deconfined quarks and gluons (QGP). Considerable efforts have been invested in the study of high-energy heavy-ion collisions to reveal the existence of this phase transition and to study the properties of strongly interacting matter in the new phase, in view of *e.g.* improving our understanding of confinement, a crucial feature of QCD. The study of quarkonium production and suppression is among the most interesting investigations in this field. Calculations indicate that the QCD with binding potential is screened in the QGP phase, the screening level increasing with energy density. Given the existence of several quarkonium states of different binding energies, it is expected that they will be consecutively dissolved (into open charm or bottom mesons) above certain energy density thresholds.

One of the objectives of high energy nuclear collisions is to produce and study the QGP under controlled conditions in the laboratory. How then can we probe the QGP - what phenomena provide us with information about its thermodynamic state? Here the ultimate aim must be to carry out *ab initio* calculations of the in-medium behaviour of the probe in finite temperature QCD. Quarkonia may well provide the best tool presently known for this. However, quarkonium production will also be modified in nuclear collisions by other phenomena. Parton distribution modifications, parton energy loss and cold nuclear matter effects on quarkonium production must be accounted for before any QGP studies become meaningful.

Any modifications observed when comparing J/ψ production in AA collisions to that in pp interactions thus have two distinct origins. Of primary interest is obviously the effect of the medium produced in the collision - this is the candidate for the QGP we want to study. In addition, however, the presence of the "normal" initial and final state effects will presumably also affect the production process and the measured rates. This ambiguity in the origin of any observed J/ψ suppression will thus have to be resolved.

A second empirical feature to be noted is that the

observed J/ψ production consists of directly produced $1S$ states as well as of decay products from $\chi_c(1P)$ and $\psi'(2S)$ production. The presence of a hot QGP affects the higher excited quarkonium states much sooner (at lower temperatures) than the ground states. This results in another ambiguity in observed J/ψ production - are only the higher excited states affected, or do all states suffer?

Ideally, one would measure J/ψ, χ_c and ψ' production separately first in pA (or dA) collisions, to determine the effects of cold nuclear matter, and then, again separately, in AA collisions as a function of collision centrality at different center-of-mass energies.

To deepen our understanding of heavy-quarkonium production mechanisms in pp and pA, we must now begin to study new observables such as associated production. As we have discussed above, theoretical uncertainties on the yields are too large to draw any strong conclusions in favour or disfavour of one model or the other. In addition, polarization studies are in practice challenging and not always possible in the complete phase-space region where one can measure the yield. Much is expected from the LHC on the latter two observables. Nonetheless, one should also use the LHC for experimental investigations of new measurements, not possible previously. These observables can test the many production models available, in particular the CSM, the COM, the CEM and the k_T factorization. The study of associated production, $\psi + c\bar{c}$, $\Upsilon + b\bar{b}$, $\psi + \gamma$, ..., first in pp collisions, then in pA and AA, should be very fruitful.

Acknowledgments

The authors appreciate and acknowledge support for this workshop and for the work on this document provided, in part or in whole, by

- the French IN2P3/CNRS;
- the ReteQuarkonii Networking of the EU I3 Hadron Physics 2 program;
- Xunta de Galicia under contract (2008/012);
- the Spanish Ministerio de Ciencia under contract FPA2008-03961-E;
- the U.S. Department of Energy under the contracts DE-AC52-07NA27344 (R. V.), DE-AC02-07CH11359 (V. P.);
- the U.S. National Science Foundation under grant NSF PHY-0555660 (R. V.);
- the German Research Foundation (DFG) under grant PI182/3-1 (B. K.);
- the Fondecyt (Chile) under grant 1090291;
- the Conicyt-DFG under grant No. 084-2009;
- the Georgian National Science Foundation grant GNSF/ST08/4-421.

References

[1] F. Abe *et al.* [CDF], Phys. Rev. Lett. **79** (1997) 572.
[2] F. Abe *et al.* [CDF], Phys. Rev. Lett. **79** (1997) 578.
[3] C-H. Chang, Nucl. Phys. B **172** (1980) 425; R. Baier, R. Rückl, Phys. Lett. B **102** (1981) 364; E. L. Berger, D. L. Jones, Phys. Rev. D **23** (1981) 1521.
[4] G. T. Bodwin, E. Braaten, G. P. Lepage, Phys. Rev. D **51** (1995) 1125 [Erratum-ibid. D **55** (1997) 5853].
[5] S. Abachi *et al.* [D0], Phys. Lett. B **370** (1996) 239.
[6] A. A. Affolder *et al.* [CDF], Phys. Rev. Lett. **85** (2000) 2886.
[7] D. Acosta *et al.* [CDF], Phys. Rev. D **71** (2005) 032001.
[8] A. Abulencia *et al.* [CDF], Phys. Rev. Lett. **99** (2007) 132001.
[9] T. Aaltonen *et al.* [CDF], Phys. Rev. D **80** (2009) 031103.
[10] A. Adare *et al.* [PHENIX], Phys. Rev. Lett. **98** (2007) 232002.
[11] S. S. Adler *et al.* [PHENIX], Phys. Rev. Lett. **92** (2004) 051802.
[12] E. T. Atomssa [PHENIX], Eur. Phys. J. C **61** (2009) 683.
[13] B. I. Abelev *et al.* [STAR], Phys. Rev. C **80** (2009) 041902.
[14] C. L. da Silva [PHENIX], Nucl. Phys. A **830** (2009) 227c.
[15] A. Adare [PHENIX], arXiv:0912.2082 [hep-ex].
[16] M. Butenschoen, these proceedings [arXiv:1011.3670 [hep-ph]].
[17] B. Gong, Z.G. He, R. Li, J.X. Wang, these proceedings.
[18] P. Artoisenet, J. M. Campbell, J. P. Lansberg, F. Maltoni, F. Tramontano, Phys. Rev. Lett. **101** (2008) 152001 .
[19] T. Affolder *et al.* [CDF], Phys. Rev. Lett. **84** (2000) 2094.
[20] D. Acosta *et al.* [CDF], Phys. Rev. Lett. **88** (2002) 161802.
[21] V. M. Abazov *et al.* [D0], Phys. Rev. Lett. **94**, 232001 (2005), [Erratum-ibid. **100**, 049902 (2008)].
[22] V. M. Abazov et al. [D0] Phys. Rev. Lett. **101** (2008) 182004.
[23] P. Artoisenet, J. P. Lansberg, F. Maltoni, Phys. Lett. B **653** (2007) 60.
[24] J. M. Campbell, F. Maltoni, F. Tramontano, Phys. Rev. Lett. **98** (2007) 252002.
[25] B. Gong, J. X. Wang, Phys. Rev. Lett. **100** (2008) 232001.
[26] B. Gong, J. X. Wang, Phys. Rev. D **78** (2008) 074011 .
[27] B. Gong, X. Q. Li, J. X. Wang, Phys. Lett. B **673** (2009) 197. [Erratum-ibid. **693**, 612 (2010)].
[28] S. Brodsky, J. P. Lansberg, Phys. Rev. D **81** (2010) 051502.
[29] J. P. Lansberg, PoS **ICHEP 2010** (2010) 206, arXiv:1012.2815 [hep-ph].
[30] M. Kramer, Nucl. Phys. B **459** (1996) 3.
[31] N. Brambilla *et al.*, Eur. Phys. J. C**71** (2011) 1534.
[32] J.P. Lansberg, Eur. Phys. J. C **60** (2009) 693.
[33] B. Gong, J. X. Wang, H. F. Zhang, arXiv:1009.3839 [hep-ph].
[34] Y. Q. Ma, K. Wang, K. T. Chao, Phys. Rev. Lett. **106** (2011) 042002.
[35] M. Butenschoen, B. A. Kniehl, arXiv:1009.5662 [hep-ph].
[36] Y. J. Zhang, Y. Q. Ma, K. Wang, K. T. Chao, Phys. Rev. D **81** (2010) 034015.
[37] P. Pakhlov *et al.* [Belle], Phys. Rev. D **79** (2009) 071101.
[38] G. C. Nayak, M. X. Liu, F. Cooper, Phys. Rev. D **68** (2003) 034003.
[39] H. S. Chung, C. Yu, S. Kim, J. Lee, Phys. Rev. D **81** (20010) 014020.
[40] J. P. Lansberg, Phys. Lett. B **695** (2011) 149.
[41] T. Dahms [CMS], talk at Quarkonium 2010.
[42] D. Price [ATLAS], these proceedings.
[43] R. Arnaldi [ALICE], talk at Hard Probes 2010.
[44] P. Robbe [LHCb], these proceedings.
[45] E. Scomparin [ALICE], these proceedings.

[46] B. Boyer [ALICE], Talk at RQW 2010, Oct. 25-28 2010, Nantes, France [slides]
[47] ATLAS Coll., **ATLAS-CONF-2010-062** (2010).
[48] CMS Coll., arXiv:1011.4193 [hep-ex].
[49] LHCb Coll., **LHCb-CONF-2010-010** (2010).
[50] B. Z. Kopeliovich, B. G. Zakharov, Phys. Rev. D **44** (1991) 3466.
[51] R. Vogt, Nucl. Phys. A **700** (2002) 539 .
[52] D. de Florian, R. Sassot, Phys. Rev. D **69** (2004) 074028.
[53] K. J. Eskola, V. J. Kolhinen, P. V. Ruuskanen, Nucl. Phys. B **535** (1998) 351.
[54] K. J. Eskola, V. J. Kolhinen, C. A. Salgado, Eur. Phys. J. C **9** (1999) 61.
[55] K. J. Eskola, H. Paukkunen, C. A. Salgado, JHEP **0807** (2008) 102.
[56] K. J. Eskola, H. Paukkunen, C. A. Salgado, JHEP **0904** (2009) 065.
[57] E. G. Ferreiro, F. Fleuret, J. P. Lansberg, A. Rakotozafindrabe, Phys. Lett. B **680** (2009) 50.
[58] S. Gavin, J. Milana, Phys. Rev. Lett. **68** (1992) 1834.
[59] T. Matsui, H. Satz, Phys. Lett. B **178** (1986) 416.
[60] B. Alessandro et al.[NA50], Eur. Phys. J. C **39** (2005) 335.
[61] R. Arnaldi et al. [NA60], Phys. Rev. Lett. **99** (2007) 132302.
[62] B. Z. Kopeliovich, Nucl. Phys. A **854** (2011) 187.
[63] B. Kopeliovich, A. Tarasov, J. Hüfner, Nucl. Phys. A **696** (2001) 669.
[64] B. Z. Kopeliovich, I. K. Potashnikova, H. J. Pirner and I. Schmidt, Phys. Rev. C **83** (2011) 014912.
[65] A. Adare *et al.* [PHENIX], Phys. Rev. C **77** (2008) 024912, Erratum-ibid. C **79** (2009) 059901.
[66] B.Z. Kopeliovich, A. Schäfer, A.V. Tarasov, Phys. Rev. D **62** (2000) 054022.
[67] M. Strikman, Nucl. Phys. A **854** (2011) 144.
[68] V. N. Gribov, Sov. Phys. JETP **29** (1969) 483 [Zh. Eksp. Teor. Fiz. **56** (1969) 892].
[69] V. A. Karmanov, L. A. Kondratyuk, Pisma Zh. Eksp. Teor. Fiz. **18**, 451 (1973).
[70] C. Lourenco, Nucl. Phys. A **610** (1996) 552c.
[71] M. Gonin, Nucl. Phys. A **610** (1996) 404c.
[72] M.C. Abreu et al., Phys. Lett. B **410** (1997) 337.
[73] E. Scomparin [NA60], Nucl. Phys. A **830**, (2009) 239c.
[74] R. Arnaldi [NA60], Nucl. Phys. A **830**, (2009) 345c.
[75] P. Cortese et al. (Na60), talk presented at the 3rd International Conference on Hard and Electromagnetic Probes of High-energy Nuclear Collisions, Illa de A Toxa, Galicia, Spain, June 8-14, 2008.
[76] J. Hüfner, B.Z. Kopeliovich, Phys. Lett. B **445** (1998) 223.
[77] F. Arleo et al., arXiv:1006.0818.
[78] J. Dolejsi, J. Hufner, B. Z. Kopeliovich, Phys. Lett. B **312** (1993) 235.
[79] M. B. Johnson, B. Z. Kopeliovich, A. V. Tarasov, Phys. Rev. C **63** (2001) 035203.
[80] K. J. Golec-Biernat, M. Wusthoff, Phys. Rev. D **60** (1999) 114023.
[81] D. M. Alde *et al.*, Phys. Rev. Lett. **66** (1991) 2285.
[82] M. J. Leitch *et al.* [FNAL E866/NuSea], Phys. Rev. Lett. **84** (2000) 3256.
[83] J. Badier *et al.* [NA3], Z. Phys. C **20** (1983) 101.
[84] B. Z. Kopeliovich, F. Niedermayer, Dubna preprint JINR-E2-84-834 [KEK Library].
[85] S. J. Brodsky, P. Hoyer, Phys. Lett. B **298** (1993) 165.
[86] B. Z. Kopeliovich, J. Nemchik, I. K. Potashnikova, M. B. Johnson, I. Schmidt, Phys. Rev. C **72** (2005) 054606.
[87] I. Abt et al. [HERA-B], Eur. Phys. J. C **60** (2009) 525.
[88] M.J. Leitch et al. [E866], Phys. Rev. Lett. **84** (2000) 3256.
[89] B. Alessandro et al. [NA50], Eur. Phys. J. C **48** (2006) 329.
[90] R. Arnaldi et al. [NA60], Eur. Phys. J. C **59** (2009) 607.
[91] R.J. Glauber et al., Lectures on theoretical physics, Inter-Science, New York, (1959) Vol. I.
[92] H. DeVries, C.W. DeJager, C. DeVries, Atomic Data and Nucl. Data Tables **36** (1987) 495.
[93] R. Vogt, Phys. Rev. C **61** (2000) 035203.
[94] H.K. Woehri, these proceedings.
[95] A. Badier et al. [NA3], Zeit. Phys. C **26** (1984) 489.
[96] K.G. Boreskov, A.B. Kaidalov, JETP Lett. D**77** (2003) 599.
[97] R. Arnaldi et al., arXiv:1004.5523, submitted to Phys. Rev. Lett.
[98] S.J. Brodsky, F. Fleuret, J.P Lansberg, to appear.
[99] A. D. Frawley, talk at ECT* workshop on Quarkonium Production in Heavy-Ion Collisions, Trento (Italy), May 25-29, 2009 and at Joint CATHIE-INT mini-program "Quarkonia in Hot QCD", June 16-26, 2009 [slides].
[100] R. Vogt, Phys. Rev. **C71**, 054902 (2005).
[101] C. Lourenco, R. Vogt, H. K. Woehri, JHEP **0902** (2009) 014.
[102] E. G. Ferreiro, F. Fleuret, J. P. Lansberg, A. Rakotozafindrabe, Phys. Rev. C **81** (2010) 064911.
[103] H. Haberzettl, J. P. Lansberg, Phys. Rev. Lett. **100** (2008) 032006; J. P. Lansberg, J. R. Cudell, Yu. L. Kalinovsky, Phys. Lett. B **633** (2006) 301.
[104] A. Adare et al. [PHENIX], arXiv:1010.1246.
[105] C. Hadjidakis [ALICE], these proceedings.
[106] H. Fujii, F. Gelis, R. Venugopalan, Nucl. Phys. A**780** (2006) 146.
[107] N. Brambilla, et al, CERN Yellow Report, CERN-2005-005, arXiv:hep-ph/0412158.
[108] M. Kramer, Prog. Part. Nucl. Phys. **47** (2001) 141.
[109] J. P. Lansberg, Int. J. Mod. Phys. A **21** (2006) 3857.
[110] J. P. Lansberg *et al.*, AIP Conf. Proc. **1038** (2008) 15.
[111] M. Beneke, I.Z. Rothstein, Phys. Lett. **B372** (1996) 157 , [Erratum-ibid. B**389** (1996) 769].
[112] M. Beneke, M. Krämer, Phys. Rev. D**55** (1997) 5269.
[113] E. Braaten, B.A. Kniehl,, J. Lee, Phys. Rev. D**62** (2000) 094005.
[114] B. A. Kniehl, J. Lee, Phys. Rev. D**62** (2000) 114027.
[115] A. K. Leibovich, Phys. Rev. D **56** (1997) 4412.
[116] P. Faccioli, C. Lourenco, J. Seixas, H. K. Wohri, Phys. Rev. Lett. **102** (2009) 151802.
[117] P. Faccioli, C. Lourenco, J. Seixas, Phys. Rev. Lett. **105** (2010) 061601.
[118] P. Faccioli, C. Lourenco, J. Seixas, Phys. Rev. D **81** (2010) 111502.
[119] P. Faccioli, C. Lourenco, J. Seixas, H. K. Wohri, Eur. Phys. J. C **69** (2010) 657.
[120] M. Butenschoen, B. A. Kniehl, arXiv:1011.5619 [hep-ph].
[121] S. P. Baranov, N. P. Zotov, JETP Lett. **86** (2007) 435.
[122] S. P. Baranov, N. P. Zotov, JETP Lett. **88** (2008) 711.
[123] CDF Coll., CDF Note 9966.
[124] P. Artoisenet, J. M. Campbell, F. Maltoni, F. Tramontano, Phys. Rev. Lett. **102** (2009) 142001.
[125] C. H. Chang, R. Li,, J. X. Wang, Phys. Rev. D **80** (2009) 034020.
[126] M. Jungst [H1 and ZEUS], arXiv:0809.4150 [hep-ex].
[127] R. Li, J. X. Wang, Phys. Lett. B **672** (2009) 51.
[128] J. P. Lansberg, Phys. Lett. B **679** (2009) 340.
[129] S. P. Baranov, these proceedings.
[130] Z. J. Ajaltouni *et al.*, "Proceedings of the workshop: HERA and the LHC workshop series on the implications of HERA for LHC physics," arXiv:0903.3861 [hep-ph].
[131] G. Corcella, K. Lipka, 'Heavy Flavours in DIS, Hadron Colliders: Working Group Summary', arXiv:1008.2281 [hep-ph], Proceedings of Science, DIS 2010.

[132] P. Nason, S. Dawson, R.K. Ellis, Nucl. Phys. B **303** (1988) 607.
[133] R. Bonciani, S. Catani, M.L. Mangano, Nucl. Phys. B **529** (1998) 424.
[134] M. Czakon, A. Mitov, G. Sterman, Phys. Rev. D **80** (2009) 074017.
[135] M. Cacciari, P. Nason, R. Vogt, Phys. Rev. Lett. **95** (2005) 122001.
[136] Yu.L. Dokshitzer, V.A. Khoze, S.I. Troian, Phys.Rev. D **53** (1996) 89.
[137] Yu.L. Dokshitzer, G. Marchesini, B.R. Webber, Nucl. Phys. B **469** (1996) 93.
[138] U. Aglietti, G. Corcella, G. Ferrera, Nucl. Phys. B **775** (2007) 162.
[139] B.R. Webber, Nucl. Phys. B **238** (1984) 492.
[140] B. Andersson, G. Gustafson, G. Ingelman, T. Sjöstrand, Phys. Rept. **97** (1983) 31.
[141] G. Corcella et al., JHEP **0101** (2001) 010.
[142] T. Sjöstrand, S. Mrenna, P. Skands, JHEP **0605** (2006) 036.
[143] S. Frixione, B.R. Webber, JHEP **0206** (2002) 029.
[144] G. Corcella, V. Drollinger, Nucl. Phys. B **730** (2005) 82.
[145] N. Armesto, L. Cunqueiro, C.A. Salgado, Eur. Phys. J. C **63** (2009) 679.
[146] N. Armesto, G. Corcella, L. Cunqueiro, C.A. Salgado, JHEP **0911** (2009) 122.
[147] I.P. Lokhtin, A.M. Snigirev, Eur. Phys. J. C **45** (2006) 211.
[148] K. Zapp, G. Ingelman, J. Rathsman, J. Stachel, U.A. Wiedemann, Eur. Phys. J. C **60** (2009) 617.
[149] T. Renk, Phys. Rev. C **78** (2008) 034908.
[150] K. Zapp, J. Stachel, U.A. Wiedemann, Phys. Rev. Lett. **103** (2009) 152302.
[151] B. Schenke, C. Gale, S. Jeon, Phys. Rev. C **80** (2009) 054913.
[152] Y. Dokshitzer, talk at Quarkonium 2010.
[153] N. Armesto, C.A. Salgado, U.A. Wiedemann, Phys. Rev. D **69** (2004) 114003.
[154] J. Adams et al, Nucl. Phys. A **757** (2005) 102.
[155] B.B. Back et al., Nucl. Phys. A **757** (2005) 28.
[156] I. Arsene et al.,Nucl. Phys. A **757** (2005) 1.
[157] K. Adcox et al., Nucl. Phys. A **757** (2005) 184.
[158] A. Adare *et al.* [PHENIX], arXiv:1005.1627 [nucl-ex].
[159] I. Garishvili [PHENIX], Nucl. Phys. A **830** (2009) 625c-626c, arXiv:0907.5479 [nucl-ex].
[160] B.I. Abelev et al. [STAR], Phys. Rev. Lett. **98** (2007) 192301.
[161] B. I. Abelev *et al.* [STAR], arXiv:0805.0364 [nucl-ex].
[162] A. D. Frawley, T. Ullrich, R. Vogt, Phys. Rep. **462** (2008) 125.
[163] M. Czakon, A. Mitov, S. Moch, Phys. Lett. B **651** (2007) 147.
[164] M. Czakon, A. Mitov, S. Moch, Nucl. Phys. B **798** (2008) 210.
[165] M. Cacciari, S. Catani, Nucl. Phys. B **617** (2001) 253.
[166] M. Cacciari, P. Nason, Phys. Rev. Lett. **89** (2002) 122003.
[167] A. Adare *et al.* [PHENIX], Phys. Rev. Lett. **103** (2009) 082002.
[168] M. M. Aggarwal *et al.* [STAR], arXiv:1007.1200 [nucl-ex].
[169] Yu.L. Dokshitzer, V.A. Khoze, S.I. Troian, J. Phys. G **17** (1991) 1602.
[170] Yu.L. Dokshitzer, F. Fabbri, V.A. Khoze, W. Ochs, Eur. Phys. J. C **45** (2006) 387.
[171] F.E. Low, Phys. Rev. **110** (1958) 974.
[172] T.H. Burnett, N.M. Kroll, Phys. Rev. Lett. **20** (1968) 86.
[173] Yu.L. Dokshitzer, these proceedings.
[174] P.B. Gossiaux, J. Aichelin, Phys. Rev. C **78** (2008) 014904.
[175] R. Baier, Yu.L. Dokshitzer, A.H. Mueller, S. Peigne, D. Schiff, Nucl. Phys. B **484** (1997) 265.
[176] J.F. Gunion, G. Bertsch, Phys. Rev. D **25** (1982) 746.
[177] T.P. Stavreva, J.F. Owens, Phys. Rev. D **79** (2009) 054017.
[178] S.J. Brodsky, P. Hoyer, C. Peterson, N. Sakai, Phys. Lett. B **93** (1980) 451.
[179] V. Abazov, et al, [D0], Phys. Lett. B **666** (2008) 435.
[180] M. Hirai, S. Kumano, T.-H. Nagai, Phys. Rev. C **76** (2007) 065207.
[181] I. Schienbein, *et al.*, Phys. Rev. D **80** (2009) 094004.
[182] S. Digal, P. Petreczky, H. Satz, Phys. Lett. B **514** (2001) 57.
[183] F. Karsch, H. Satz, Z. Phys. C **51** (1991) 209.
[184] S. Gupta, H. Satz, Phys. Lett. B **283** (1992) 439.
[185] S. Digal, P. Petreczky, H. Satz, Phys. Rev. **D64** (2001) 094015.
[186] F. Karsch, D. Kharzeev, H. Satz, Phys. Lett. B **637**(2006) 75.
[187] F. Karsch, R. Petronzio, Phys. Lett. B **212** (1988) 255.
[188] S. Gavin, M. Gyulassy, Phys. Lett. B **214** (1988) 241.
[189] J. Hüfner, Y. Kurihara, H. J. Pirner, Phys. Lett. B **215** (1988) 218.
[190] D. Kharzeev, M. Nardi, H. Satz, Phys. Lett. B **405** (1997) 14.
[191] M. C. Abreu et al.(NA50), Nucl. Phys. A**698** (2002) 127c.
[192] P. Braun-Munzinger, J. Stachel, Nucl. Phys. A **690** (2001) 119.
[193] R. L. Thews, M. Schroedter, J. Rafelski, Phys. Rev. C **63** (2001) 054905.
[194] L. Grandchamp, R. Rapp, Nucl. Phys. A **709** (2002) 415.
[195] M. Mangano, R. L. Thews et al., Phys. Rev. C **73** (2006) 014904.
[196] A. C. Kraan, AIP Conf. Proc. **1038** (2008) 45, arXiv:0807.3123 [hep-ex].
[197] C. Albajar *et al.* [UA1], Phys. Lett. B **200** (1988) 380.
[198] C. Albajar *et al.* [UA1], Phys. Lett. B **256** (1991) 112.
[199] K. Abe *et al.* [Belle], Phys. Rev. Lett. **89** (2002) 142001.
[200] P. Artoisenet, "Proceedings of 9th Workshop on Non-Perturbative Quantum Chromodynamics, Paris, France, 4-8 Jun 2007", pp 21. arXiv:0804.2975 [hep-ph].
[201] M. Klasen, J. P. Lansberg, Nucl. Phys. Proc. Suppl. **179-180** (2008) 226.
[202] P. Artoisenet, F. Maltoni, T. Stelzer, JHEP **0802** (2008) 102.
[203] J. Alwall, P. Demin, S. de Visscher *et al.*, JHEP **0709** (2007) 028.